Advances in Nano Research, *Vol. 16, No. 3 (2024) 273-288*
https://doi.org/10.12989/anr.2024.16.3.273

Comprehensive study of internal modals interactions: Comparison of various axial nonlinear beam theories

Somaye Jamali Shakhlavi*[1,2] and Reza Nazemnezhad[1]

[1]*School of Engineering, Damghan University, Damghan, Iran*
[2]*School of Mechanical Engineering, Iran University of Science and Technology, Tehran, Iran*

(*Received April 20, 2021, Revised August 16, 2023, Accepted January 28, 2024*)

Abstract. The geometrical nonlinear vibrations of the gold nanoscale rod are investigated for the first time by considering the internal modals interactions using different nonlinear beam theories. This phenomenon is usually one of the important features of nonlinear vibration systems. For a more detailed analysis, the von-Kármán effects, preserving all the nonlinear terms in the strain-displacement relationships of gold nanoscale rods in three displacement directions, are considered to analyze the nonlinear axial vibrations of gold nanoscale rods. It uses highly accurate analytical-numerical solutions for the clamped-clamped and clamped-free boundary conditions of nanoscale gold rods. Also, with the help of Hamilton's principle, the governing equation and boundary conditions are derived based on Eringen's theory. The influence of nonlinear and nonlocal factors on axial vibrations was investigated separately for all three theories: Simple (ST), Rayleigh (RT) and Bishop (BT). Using different theories, the effects of inertia and shear on the internal resonances of gold nanorods were studied and compared in terms of two-to-one and three-to-one internal resonances. As the nonlocal parameter of the gold nanorod increases, the maximum nonlinear amplitude occurs. So, by adding nonlocal effects in a gold nanorod, the internal modal interactions resulting from the unique structure can be enhanced. It is worth noting that shear and inertial analysis have a significant effect on internal modal interactions in gold nanorods.

Keywords: gold nanoscale rod; internal modals interactions; nonlinear axial vibrations; nonlocal theory

1. Introduction

One of the novel ideas in medicine is the use of nanoparticles in the diagnosis and treatment of a number of common cancers. Due to the diversity in structure and unique properties of nanoscale materials, including optical, electronic, magnetic and catalytic properties, nanoparticles can be utilized in imaging, diagnosis and treatment of cancers (Morton *et al*. 2010). Gold nanoparticles are significant among nanoparticles due to their surface functional characteristics and the ability to generate heat due to light, Abadeer and Murphy (2016). Due to the phenomenon of Surface Plasmon Resonance (mass movement of conductive electrons), gold nanoparticles strongly absorb light and convert it into thermal energy. Therefore, when a small mass of gold particles is excited by a certain frequency of the laser, they begin to heat the field with a radius a thousand times larger than their size, which generates heat that hits the tumor cells and destroys them. Nanoscale gold rods are one form of gold nanoparticles. Gold nanorods have many advantages for use in therapy. One of them is that they have 20 times or more light absorption than other forms of gold nanoparticles. They also have two aspects of longitudinal and transverse surface Plasmon resonance and have a higher ability to absorb the light of their longitudinal Plasmon resonance. The wave-length of light at which longitudinal resonance occurs is controlled by the aspect ratio of the nanoscale rods (Hainfeld *et al*. 2010, Miller *et al*. 2016). Since the dimensions of gold nanoscale rods are very important for their therapeutic effect, in this research based on valid medical data (Saha *et al*. 2012), it has been tried to use the optimal dimensions to check its mechanical properties, especially the extraction of its internal resonances, which have a great effect on the destruction of cancer cells. In the present study, gold nanoscale rods were utilized for the above reasons. And all its mechanical properties, including linear and nonlinear frequencies, linear mode shape, frequency variations based on length, diameter, mode shape, aspect ratio of the nanoscale rods, and useful internal resonance rods of nanoscale gold have been thoroughly evaluated to fit unique geometries. Since this research is also very important in terms of mechanical engineering, in this section, additional explanations are provided in this field. Nanotechnology is one of the most important issues. Nanoscale rods are central to many applications at the nano-length scale like, Shakhlavi and Nazemnezhad (2024), Shakhlavi *et al.* (2020, 2021a, b, 2022a, b), Shakhlavi (2023, 2024), Amabili (2018). Single-layer and double-layer nanorods are used in various nano-electromechanical systems and materials science. Understanding the mechanical behavior of nanoscale rods is an important issue for efficient design. The mechanics of nanostructures usually depends on their size. Size dependence disappears with increasing dimensions. Various nonlocal elasticity theories were proposed to account for the size-dependent behavior of nanostructures.

*Corresponding author, Ph.D.,
E-mail: So_jamali@mecheng.iust.ac.ir

ISSN: 2287-237X (Print), 2287-2388 (Online)

A stress-type nonlocal elasticity model is presented by Eringen (1983, 1976). In this model, it is assumed that the stress at a reference point is a function of the strain field at any point of the continuum. The interactions of the nearest atoms in the elastic body are considered by it. Eringen (1976) used lattice dynamic effects in unidirectional wave propagation at the end of the first Brillouin zone to validate his nonlocal stress gradient theory.

Recently, the bending, buckling, and wave propagation of Eltaher *et al*. (2016) and torsional Shakhlavi, Hosseini-Hashemi, and Nazemnezhad (2020) in nanostructures have been investigated using nonlocal elasticity theory. In the field of axial vibration analysis, extensive studies have been carried out which the most relevant ones are discussed in the following, such as: the longitudinal vibration of embedded nanorods under the influence of a transverse magnetic field was analyzed based on the non-local elastic continuum theory by Murmu, Adhikari, and McCarthy (2014). Nonlinear axial vibrations of rods are presented by Mousavi and Fariborz (2012) using the theory of elasticity. The axial vibration of nanorods modeled on the basis of the simplest rod theory using the nonlocal elastic theory was studied by Aydogdu (2009). Kiani (2010) evaluated the effect of small scale on free axial vibration of nanowires in terms of linear variable radii. It also uses the simplest rod theory to model tapered nanorods. A similar study on the axial vibration of two nanorod systems is also found by Murmu and Adhikari (2010). Crack effects were also studied considering the nonlocal theory of Hsu, Lee, and Chang (2011) on the longitudinal vibration of nanobeams. Also, the aforementioned effect was investigated on longitudinal wave propagation analysis of coupled nanorod systems by Narendar and Gopalakrishnan (2011). The effect of small scale on the axial vibration of non-uniform nanorods was evaluated by using the boundary characteristic orthogonal polynomial by Faroughi and Goushegir (2016). The rod model was used by Aydogdu (2015) to model the axial vibration of double-walled carbon nanotubes. In the mentioned research, the van der Waals forces were weighted in the axial direction and the effect of the small scale on the natural axial frequencies of the nanotubes was investigated. Nonlocal longitudinal vibration of viscoelastically coupled double nanorod systems was investigated by (Karličić *et al*. 2015). Finally, there are only a few researches that use the Bishop model to analyze the behavior of thick nanoscale rods like: Nazemnezhad and Kamali (2018a, b), Nazemnezhad *et al*. (2019), Li *et al*. (2017), Güven (2014). These studies have considered a homogeneous rod and a functionally graded rod for linear nanostructures. Among other things that can be mentioned is the use of continuum models in lattice-like materials for enhanced lattice prediction with next-nearest interactions, Gómez-Silva and Zaera (2022a, b, c), Bacigalupo and Gambarotta (2019), Bacigalupo and Gambarotta (2021). In the mentioned history, it has been tried to pay more attention to the new researches related to axial vibrations with different topics. The important point is that in all the mentioned researches, the analysis was done only theoretically. In this research, firstly, it has been tried to present a new work in terms of theory, and secondly, by providing useful results, it has also taken into account the characteristics of the aspect of nanostructure construction.

Theory description: It is obvious that so far, no research has been done to achieve shear and inertial effects on nonlinear nonlocal axial vibrations of nanoscale rods by considering internal resonances. Since the analysis of linear and nonlinear frequencies changes based on the dimensions of structures such as nano, micro and macro structures and has different applications, therefore it is considered in this paper. Considering that before this research, no study has been done to investigate the effects of shear and inertia on the nonlocal nonlinear axial vibrations of nanoscale rods with these features, which are very useful in the manufacture of nanoscale tools. Also, due to their mechanical properties, they have been widely used as nano-electrical and nanomechanical systems such as sensors, actuators, fluid transducers, and drug delivery. Hence, the influence of the nonlocal nonlinear parameter on the axial vibrations of nanoscale rods by considering the internal resonances with numerical examples in terms of Bishop's theory has been fully analyzed in this paper.

Practical description: i) As an advantage of providing diverse geometries of nanoscale rods and the precise range of their internal resonances exposed to axial vibrations, they are very useful for the design and fabrication of nanostructures under external forces. ii) Extracting the internal resonances of gold nanoscale rods improves the treatment of diseases such as cancer, because with the occurrence of these resonances, their light absorption power increases, and as a result, tumor cells are destroyed faster. Consequently, knowing the number of internal modal interactions of each gold nanorod with a given length and the nonlocal effects on nanoparticle dimensions in terms of these internal resonances will certainly improve the recovery process.

This new study comprehensively investigates the effects of nonlocal as well as geometrical nonlinearity on the mechanics of nanoscale gold rods with large deformations through a nonlocal elasticity model to account for internal resonances. Considering both nonlocality and geometrical nonlinearity leads to a more general scale-dependent model for nanoscale gold rods. Moreover, the proposed model can be utilized in a wide range of lengths because it includes the stiffness behavior with weak hardening effects. Also, nonlocal nonlinear analysis of NEMS (Nano-Electro-Mechanical Systems) rod-type structural components is a subject of major interest in engineering and medical sciences. As a nonlocal and nonlinear geometric models, Eringen and von-Kármán theories are used in the analysis. The nonlocal nonlinear equations of gold nanostructures are presented using Hamilton's principle with a rod model. A solution approach is developed with the application of a decomposition-based procedure in conjunction with the MSM-based and HDQ methods. The relations of internal modal interactions for the gold nanorod model are also obtained based on the Multi Galerkin method. The importance of many parameters, including the size parameter, inertial and shear effects, aspect ratio of gold nanorods, as well as nonlinear effects in the size-dependent mechanics of internal resonances of nanorods with large deformations are detailed for all beam-axis theories.

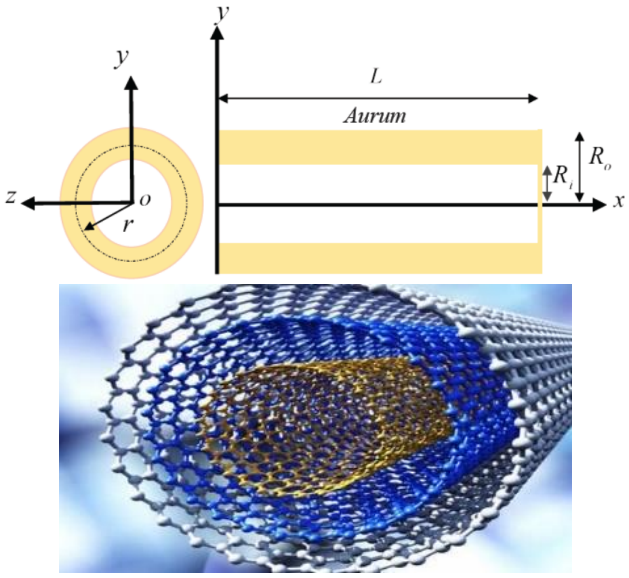

Fig 1. Gold nanoscale rod geometry

2. Theoretical formulation

Consider a nanoscale gold rod of length L, where R_i, R_o, ρ, and A denote the inner diameter, outer diameter, density, and cross-sectional area, respectively. The inner and outer surfaces are made of the same material as shown in Fig. 1.

This study considered the analysis of nonlinear free axial vibrations of homogeneous nanoscale rods in the presence of nonlocal effects. According to Bishop's theory specified for the axial vibrations of thick rods in the nanoscale, the displacement field is written as follows, Rao (2019).

$$u = u(x,t); \quad v = -\upsilon y \frac{\partial u(x,t)}{\partial x}; \quad w = -\upsilon z \frac{\partial u(x,t)}{\partial x} \quad (1)$$

where u, v, w and υ are displacement components along x, y, z axes and Poisson's ratio, respectively. The relationship of Von-Kármán strain-displacement with the nonlinear terms is as (Eq. (2)).

The strain relationships are derived by substituting Eq. (1) into Eq. (2), i.e., as (Eq. (3)).

And the corresponding stresses can be written as Eq. (4).

So, in the Eq. (4), λ, and $G$are Lame's constants as Eq. (5).

With the help of the equations in terms of strain and stress components for the nanoscale rod, now it is possible to derive the nonlocal-nonlinear governing equations of the motions and the corresponding boundary conditions. To this regard, the variational approach is used. The variational approach needs the strain$\delta U$and the kineticδTenergies of the nanoscale-rod that they are determined as Eqs. (6) and (7), respectively.

In the Eq. (7), $\rho(r)[kg/m^3]$ and $V[m^3]$ showman the density and the nanoscale rod volume, respectively. Using Hamilton's principle and performance some mathematical operations generate the nonlinear governing equations of motion and boundary conditions as Eqs. (8) and (9).

Where N_{xx}, N_{yy}, N_{zz}, M_{xy}, and M_{xz} are the stress resultants, determined as Eqs. (10)-(14).

The governing Eqs. (8)-(9) represent the classical form. Therefore, to achieve the nanoscale form, Eringen's model was used to analyze the size-dependent effects on the axial vibration behavior of nanoscale rods. Since Eringen's model is more practical than other theories (such as: surface elasticity theory, strain gradient theory, couple stress theory, and modified couple stress theory), consequently, it encourages authors to investigate the size-dependent behavior of nanoscale rods applying nonlocal elastic theory.

$$\varepsilon_{ij} = \frac{1}{2}\Big(\underbrace{u_{i,j} + u_{j,i}}_{Linear\ \ term} + \underbrace{u_{m,i}u_{m,j}}_{von-karman\ \ term}\Big) \Rightarrow (a)$$

$$Suppose \Rightarrow identifiers\ \ are\ \ i,j,m \Rightarrow \begin{cases} i = x,y,z \\ j = x,y,z \\ m = x,y,z \end{cases}$$

$$For\ \ example,\ \ for\ \ identifier\ \ i = j = x,$$

$$Eq.(a)\ \ was\ \ expanded\ \ as\ \ follows$$

$$\varepsilon_{xx} = \frac{1}{2}\left(u_{x,x} + u_{x,x} + u_{m,x}u_{m,x}\right)$$

$$\varepsilon_{xx} = \left[\frac{1}{2}\left(\frac{\partial u_x}{\partial x} + \frac{\partial u_x}{\partial x} + \frac{\partial u_m}{\partial x}\frac{\partial u_m}{\partial x}\right) = \right.$$

$$\left. \frac{1}{2}\left(\frac{\partial u_x}{\partial x} + \frac{\partial u_x}{\partial x} + \frac{\partial u_x}{\partial x}\frac{\partial u_x}{\partial x} + \right.\right.$$

$$\left.\left. \frac{\partial u_y}{\partial x}\frac{\partial u_y}{\partial x} + \frac{\partial u_z}{\partial x}\frac{\partial u_z}{\partial x}\right)\right] \quad (2)$$

$$\varepsilon_{xx} = \left[\frac{1}{2}\left(2\frac{\partial u_x}{\partial x} + \frac{\partial u_x}{\partial x}\frac{\partial u_x}{\partial x} + \right.\right.$$

$$\left.\left. \underbrace{\frac{\partial u_y}{\partial x}\frac{\partial u_y}{\partial x}}_{0} + \underbrace{\frac{\partial u_z}{\partial x}\frac{\partial u_z}{\partial x}}_{0}\right)\right]$$

$$= \frac{\partial u_x}{\partial x} + \frac{1}{2}\left(\frac{\partial u_x}{\partial x}\right)^2$$

$$\varepsilon_{xx} = \frac{\partial u}{\partial x} + \frac{1}{2}\left(\frac{\partial u}{\partial x}\right)^2$$

$$\varepsilon_{yy} = \varepsilon_{zz} = -\upsilon\frac{\partial u}{\partial x} + \frac{1}{2}\upsilon^2\left(\frac{\partial u}{\partial x}\right)^2$$

$$\varepsilon_{xy} = -\frac{1}{2}\upsilon y\frac{\partial^2 u}{\partial x^2} + \frac{1}{2}\upsilon^2 y\frac{\partial u}{\partial x}\left(\frac{\partial^2 u}{\partial x^2}\right) \quad (3)$$

$$\varepsilon_{xz} = -\frac{1}{2}\upsilon z\frac{\partial^2 u}{\partial x^2} + \frac{1}{2}\upsilon^2 z\frac{\partial u}{\partial x}\left(\frac{\partial^2 u}{\partial x^2}\right)$$

$$\varepsilon_{yz} = 0$$

$$\sigma_{xx} = (\lambda(1-2\upsilon) + 2G)\frac{\partial u}{\partial x} + \left(\lambda\left(\frac{1}{2} + \upsilon^2\right) + G\right)\left(\frac{\partial u}{\partial x}\right)^2$$

$$\sigma_{yy} = \sigma_{zz} = \left(\lambda\left(\frac{1}{2} + \upsilon^2\right) + G\upsilon^2\right)\left(\frac{\partial u}{\partial x}\right)^2$$

$$\sigma_{xy} = -G\upsilon y\frac{\partial^2 u}{\partial x^2} + G\upsilon^2 y\frac{\partial u}{\partial x}\left(\frac{\partial^2 u}{\partial x^2}\right) \quad (4)$$

$$\sigma_{xz} = -G\upsilon z\frac{\partial^2 u}{\partial x^2} + G\upsilon^2 z\frac{\partial u}{\partial x}\left(\frac{\partial^2 u}{\partial x^2}\right)$$

$$\sigma_{yz} = 0$$

$$\lambda = \frac{E\upsilon}{(1+\upsilon)(1-2\upsilon)}, \qquad G = \frac{E}{2(1+\upsilon)} \quad (5)$$

$$\delta U = \int\left[\begin{matrix}(\sigma_{xx}\delta\varepsilon_{xx} + \sigma_{yy}\delta\varepsilon_{yy} + \sigma_{zz}\delta\varepsilon_{zz} + \\ \sigma_{xy}\delta\gamma_{xy} + \sigma_{xz}\delta\gamma_{xz} + \sigma_{yz}\delta\gamma_{yz})\end{matrix}\right] dV \quad (6)$$

$$,\gamma_{xy} = 2\varepsilon_{xy}$$

$$\delta T = \rho \int (\dot{u}_x\, \delta\dot{u}_x + \dot{u}_y \delta\dot{u}_y + \dot{u}_z \delta\dot{u}_z) dV \tag{7}$$

$$\begin{aligned}
&-\frac{\partial}{\partial x}(N_{xx}) - \frac{\partial}{\partial x}\left(N_{xx}\frac{\partial u}{\partial x}\right) + \frac{\partial}{\partial x}\left(\upsilon N_{yy}\right) \\
&-\frac{\partial}{\partial x}\left(\upsilon^2 N_{yy}\frac{\partial u}{\partial x}\right) + \frac{\partial}{\partial x}(\upsilon N_{zz}) \\
&-\frac{\partial}{\partial x}(\upsilon^2 N_{zz}\frac{\partial u}{\partial x}) - \frac{\partial^2}{\partial x^2}(\upsilon M_{xy}) - \\
&\frac{\partial}{\partial x}(\upsilon^2 M_{xy}\frac{\partial^2 u}{\partial x^2}) + \frac{\partial^2}{\partial x^2}(\upsilon^2 M_{xy}\frac{\partial u}{\partial x}) - \frac{\partial^2}{\partial x^2}(\upsilon M_{xz}) \\
&-\frac{\partial}{\partial x}(\upsilon^2 M_{xz}\frac{\partial^2 u}{\partial x^2}) + \frac{\partial^2}{\partial x^2}(\upsilon^2 M_{xz}\frac{\partial u}{\partial x}) + \rho A\frac{\partial^2 u}{\partial t^2} \\
&-\upsilon^2 I_p \rho \frac{\partial^4 u}{\partial x^2 \partial t^2} = 0
\end{aligned} \tag{8}$$

Subjected to,

$$\left[\begin{pmatrix} N_{xx} + N_{xx}\frac{\partial u}{\partial x} - \upsilon N_{yy} + \upsilon^2 N_{yy}\frac{\partial u}{\partial x} - \upsilon N_{zz} \\ +\upsilon^2 N_{zz}\frac{\partial u}{\partial x} + \frac{\partial}{\partial x}(\upsilon M_{xy}) + \upsilon^2 M_{xy}\frac{\partial^2 u}{\partial x^2} \\ -\frac{\partial}{\partial x}\left(\upsilon^2 M_{xy}\frac{\partial u}{\partial x}\right) + \frac{\partial}{\partial x}(\upsilon M_{xz}) + \upsilon^2 M_{xz}\frac{\partial^2 u}{\partial x^2} \\ -\frac{\partial}{\partial x}\left(\upsilon^2 M_{xz}\frac{\partial u}{\partial x}\right) + \rho\upsilon^2 I_p \frac{\partial^3 u}{\partial x \partial t^2} \end{pmatrix}_{(\delta u)}\right]_0^L = 0$$

$$\left[\left(-\upsilon M_{xy} + \upsilon^2 M_{xy}\frac{\partial u}{\partial x} - \upsilon M_{xz} + \upsilon^2 M_{xz}\frac{\partial u}{\partial x}\right)_{(\delta u')}\right]_0^L = 0 \tag{9}$$

$$N_{xx} = \int \sigma_{xx} dA = \int \begin{pmatrix} (\lambda(1-2\upsilon) + 2G)\frac{\partial u}{\partial x} + \\ \left(\lambda\left(\frac{1}{2} + \upsilon^2\right) + G\right)\left(\frac{\partial u}{\partial x}\right)^2 \end{pmatrix} dA \tag{10}$$

$$N_{yy} = \int \sigma_{yy}\, dA = \int \left(\lambda\left(\frac{1}{2} + \upsilon^2\right) + G\upsilon^2\right)\left(\frac{\partial u}{\partial x}\right)^2 dA \tag{11}$$

$$N_{zz} = \int \sigma_{zz} dA = \int \left(\lambda\left(\frac{1}{2} + \upsilon^2\right) + G\upsilon^2\right)\left(\frac{\partial u}{\partial x}\right)^2 dA \tag{12}$$

$$\begin{aligned} M_{xy} &= \int y\sigma_{xy}\, dA \\ &= \int y\left(-G\upsilon y\frac{\partial^2 u}{\partial x^2} + G\upsilon^2 y\frac{\partial u}{\partial x}\left(\frac{\partial^2 u}{\partial x^2}\right)\right) dA \end{aligned} \tag{13}$$

$$\begin{aligned} M_{xz} &= \int z\sigma_{xz}\, dA \\ &= \int z\left(-G\upsilon z\frac{\partial^2 u}{\partial x^2} + G\upsilon^2 z\frac{\partial u}{\partial x}\left(\frac{\partial^2 u}{\partial x^2}\right)\right) dA \end{aligned} \tag{14}$$

The present study uses the differential model of nonlocal elasticity theory. The differential theory of nonlocal elasticity shows that the nonlocal state of each parameter can be obtained by multiplying the parameter by $(1-\mu\nabla^2)$, where μ is the nonlocal Coefficient, and $\nabla^2 = \frac{\partial^2}{\partial x^2} + \frac{\partial^2}{\partial y^2} + \frac{\partial^2}{\partial z^2}$ is the Laplacian operator. Now, according to the statement of the nonlocal elasticity theory, the nonlocal form of Eqs. (8)-(9) are derived as Eqs. (15) and (16).

where in the Eqs. (15)-(16), N_{xx}^{nl}, N_{yy}^{nl}, N_{zz}^{nl}, M_{xy}^{nl}, and M_{xz}^{nl}, are the nonlocal stress resultants determined as Eqs. (17)-(21).

By substituting the nonlocal stress results determined in Eqs. (17) - (21) into Eqs. (15) - (16) as shown Eq. (22), the nonlinear nonlocal equation of axial free vibration for a nanoscale rod is obtained.

$$\begin{aligned}
&-\frac{\partial}{\partial x}(1-\mu\nabla^2)N_{xx}^{nl} - \frac{\partial}{\partial x}((1-\mu\nabla^2)N_{xx}^{nl}\frac{\partial u}{\partial x}) + \\
&\frac{\partial}{\partial x}(\upsilon(1-\mu\nabla^2)N_{yy}^{nl}) - \frac{\partial}{\partial x}(\upsilon^2(1-\mu\nabla^2)N_{yy}^{nl}\frac{\partial u}{\partial x}) \\
&+\frac{\partial}{\partial x}(\upsilon(1-\mu\nabla^2)N_{zz}^{nl}) - \frac{\partial}{\partial x}(\upsilon^2(1-\mu\nabla^2)N_{zz}^{nl}\frac{\partial u}{\partial x}) \\
&-\frac{\partial^2}{\partial x^2}(\upsilon(1-\mu\nabla^2)M_{xy}^{nl}) - \frac{\partial}{\partial x}(\upsilon^2(1-\mu\nabla^2)M_{xy}^{nl}\frac{\partial^2 u}{\partial x^2}) \\
&+\frac{\partial^2}{\partial x^2}(\upsilon^2(1-\mu\nabla^2)M_{xy}^{nl}\frac{\partial u}{\partial x}) - \frac{\partial^2}{\partial x^2}(\upsilon(1-\mu\nabla^2)M_{xz}^{nl}) \\
&-\frac{\partial}{\partial x}(\upsilon^2(1-\mu\nabla^2)M_{xz}^{nl}\frac{\partial^2 u}{\partial x^2}) + \frac{\partial^2}{\partial x^2}(\upsilon^2(1-\mu\nabla^2)M_{xz}^{nl}\frac{\partial u}{\partial x}) \\
&+\rho A(1-\mu\nabla^2)\frac{\partial^2 u}{\partial t^2} - \upsilon^2 I_p \rho(1-\mu\nabla^2)\frac{\partial^4 u}{\partial x^2 \partial t^2} = 0
\end{aligned} \tag{15}$$

Subjected to,

$$\left[\begin{pmatrix} (1-\mu\nabla^2)N_{xx}^{nl} + (1-\mu\nabla^2)N_{xx}^{nl}\frac{\partial u}{\partial x} \\ -\upsilon(1-\mu\nabla^2)N_{yy}^{nl} + \upsilon^2(1-\mu\nabla^2)N_{yy}^{nl}\frac{\partial u}{\partial x} \\ -\upsilon(1-\mu\nabla^2)N_{zz}^{nl} + \upsilon^2(1-\mu\nabla^2)N_{zz}^{nl}\frac{\partial u}{\partial x} + \\ \frac{\partial}{\partial x}\left(\upsilon(1-\mu\nabla^2)M_{xy}^{nl}\right) + \upsilon^2(1-\mu\nabla^2)M_{xy}^{nl}\frac{\partial^2 u}{\partial x^2} \\ -\frac{\partial}{\partial x}\begin{pmatrix}\upsilon^2(1-\mu\nabla^2) \\ * M_{xy}^{nl}\frac{\partial u}{\partial x}\end{pmatrix} + \frac{\partial}{\partial x}\begin{pmatrix}\upsilon(1-\mu\nabla^2) \\ * M_{xz}^{nl}\end{pmatrix} \\ +\upsilon^2(1-\mu\nabla^2)M_{xz}^{nl}\frac{\partial^2 u}{\partial x^2} - \frac{\partial}{\partial x}\begin{pmatrix}\upsilon^2(1-\mu\nabla^2) \\ * M_{xz}^{nl}\frac{\partial u}{\partial x}\end{pmatrix} \\ +\rho\upsilon^2 I_p(1-\mu\nabla^2)\frac{\partial^3 u}{\partial x \partial t^2} \end{pmatrix}_{(\delta u)}\right]_0^L = 0$$

$$\left[\begin{pmatrix} -\upsilon(1-\mu\nabla^2)M_{xy}^{nl} + \upsilon^2(1-\mu\nabla^2)M_{xy}^{nl}\frac{\partial u}{\partial x} - \\ \upsilon(1-\mu\nabla^2)M_{xz}^{nl} + \upsilon^2(1-\mu\nabla^2)M_{xz}^{nl}\frac{\partial u}{\partial x} \end{pmatrix}_{(\delta u')}\right]_0^L = 0 \tag{16}$$

$$(1-\mu\nabla^2)N_{xx}^{nl} = N_{xx} = \int \begin{pmatrix} (\lambda(1-2\upsilon) + 2G)\frac{\partial u}{\partial x} \\ +\left(\lambda\left(\frac{1}{2} + \upsilon^2\right) + G\right)\left(\frac{\partial u}{\partial x}\right)^2 \end{pmatrix} dA \tag{17}$$

$$(1-\mu\nabla^2)N_{yy}^{nl} = N_{yy} = \int \left(\lambda\left(\frac{1}{2} + \upsilon^2\right) + G\upsilon^2\right)\left(\frac{\partial u}{\partial x}\right)^2 dA \tag{18}$$

$$(1-\mu\nabla^2)N_{zz}^{nl} = N_{zz} = \int \left(\lambda\left(\frac{1}{2} + \upsilon^2\right) + G\upsilon^2\right)\left(\frac{\partial u}{\partial x}\right)^2 dA \tag{19}$$

$$(1-\mu\nabla^2)M_{xy}^{nl} = M_{xy} = \int y\begin{pmatrix} -G\upsilon y\frac{\partial^2 u}{\partial x^2} + \\ G\upsilon^2 y\frac{\partial u}{\partial x}\left(\frac{\partial^2 u}{\partial x^2}\right) \end{pmatrix} dA \tag{20}$$

$$(1-\mu\nabla^2)M_{xz}^{nl}=M_{xz}=\int z\begin{pmatrix}-G\upsilon z\dfrac{\partial^2 u}{\partial x^2}+\\ G\upsilon^2 z\dfrac{\partial u}{\partial x}\left(\dfrac{\partial^2 u}{\partial x^2}\right)\end{pmatrix}dA \tag{21}$$

$$\begin{aligned}&-AZ_1\frac{\partial^2 u}{\partial x^2}+(4\upsilon AZ_4-2AZ_2-2AZ_1)\frac{\partial u}{\partial x}\frac{\partial^2 u}{\partial x^2}-\\&(3AZ_2+6A\upsilon^2 Z_4)\frac{\partial^2 u}{\partial x^2}(\frac{\partial u}{\partial x})^2+\upsilon^2 I_p G\frac{\partial^4 u}{\partial x^4}-\\&4\upsilon^3 I_p G\frac{\partial^2 u}{\partial x^2}\frac{\partial^3 u}{\partial x^3}-2\upsilon^3 I_p G\frac{\partial u}{\partial x}\frac{\partial^4 u}{\partial x^4}+\upsilon^4 I_p G\left(\frac{\partial^2 u}{\partial x^2}\right)^3\\&+4\upsilon^4 I_p G\frac{\partial u}{\partial x}\frac{\partial^2 u}{\partial x^2}\frac{\partial^3 u}{\partial x^3}+\upsilon^4 I_p G\frac{\partial^4 u}{\partial x^4}(\frac{\partial u}{\partial x})^2+\\&\rho A\frac{\partial^2 u}{\partial t^2}-\left(\rho\upsilon^2 I_p+\mu A\rho\right)\frac{\partial^4 u}{\partial x^2\partial t^2}+\mu\rho\upsilon^2 I_p\frac{\partial^6 u}{\partial x^4\partial t^2}=0\end{aligned} \tag{22}$$

And also, the corresponding boundary condition as Eq. (23),

$$\left[\begin{pmatrix}AZ_1\dfrac{\partial u}{\partial x}+(AZ_1+AZ_2-2\upsilon AZ_4)\left(\dfrac{\partial u}{\partial x}\right)^2\\+(AZ_2+2\upsilon^2 AZ_4)\left(\dfrac{\partial u}{\partial x}\right)^3-\upsilon^2 I_p G\dfrac{\partial^3 u}{\partial x^3}\\+\upsilon^3 I_p G\left(\dfrac{\partial^2 u}{\partial x^2}\right)^2+2\upsilon^3 I_p G\dfrac{\partial u}{\partial x}\dfrac{\partial^3 u}{\partial x^3}-\\\upsilon^4 I_p G\dfrac{\partial u}{\partial x}\left(\dfrac{\partial^2 u}{\partial x^2}\right)^2-\upsilon^4 I_p G\dfrac{\partial^3 u}{\partial x^3}\left(\dfrac{\partial u}{\partial x}\right)^2\\+\rho\upsilon^2 I_p\dfrac{\partial^3 u}{\partial x\partial t^2}-\mu\upsilon^2 I_p\rho\dfrac{\partial^5 u}{\partial x^3\partial t^2}\end{pmatrix}\delta u+\begin{pmatrix}\upsilon^2 I_p G\dfrac{\partial^2 u}{\partial x^2}-2\upsilon^3 I_p G\dfrac{\partial u}{\partial x}\dfrac{\partial^2 u}{\partial x^2}+\\\upsilon^4 I_p G\dfrac{\partial^2 u}{\partial x^2}\left(\dfrac{\partial u}{\partial x}\right)^2\end{pmatrix}\delta u'\right]_0^L=0 \tag{23}$$

In the Eqs. (22)-(23), the parameters are determined as follows

$$\begin{aligned}&Z_1=\lambda(1-2\upsilon)+2G;\quad Z_2=\lambda\left(\frac{1}{2}+\upsilon^2\right)+G\\&Z_4=\lambda\left(\frac{1}{2}+\upsilon^2\right)+G\upsilon^2\end{aligned} \tag{24}$$

2.1 Linear-nonlocal axial free vibrations

To study free axial vibrations in terms of nanoscale rods a harmonic equation for axial displacement is determined as Eq. (25),

$$u(x,t)=U(x)e^{i\omega t} \tag{25}$$

where ω is the linear axial frequencies of the nanoscale rod. By putting the harmonic displacement (25) in Eqs. (22)-(23) (by removing the nonlinear terms of the equations), the following equations are derived as

$$\begin{aligned}&\frac{d}{dx}\left(EA\frac{dU(x)}{dx}\right)-\frac{d^2}{dx^2}\left(\upsilon^2 GI_p\frac{d^2U(x)}{dx^2}\right)+\rho A\omega^2 U(x)\\&-\mu\omega^2\frac{d^2}{dx^2}\left(\rho AU(x)\right)-\frac{d}{dx}\left(\rho\upsilon^2 I_p\omega^2\frac{dU(x)}{dx}\right)+\\&\mu\frac{d^3}{dx^3}\left(\rho\upsilon^2 I_p\omega^2\frac{dU(x)}{dx}\right)=0\end{aligned} \tag{26}$$

Subjected to,

$$\left[\begin{pmatrix}EA\dfrac{dU(x)}{dx}-\dfrac{d}{dx}\left(\upsilon^2 GI_p\dfrac{d^2U(x)}{dx^2}\right)\\-\rho\upsilon^2 I_p\omega^2\dfrac{dU(x)}{dx}\\+\mu\dfrac{d^2}{dx^2}\left(\rho\upsilon^2 I_p\omega^2\dfrac{dU(x)}{dx}\right)\end{pmatrix}\delta U+\left(\upsilon^2 GI_p\frac{d^2U(x)}{dx^2}\right)\delta U'\right]_0^L=0 \tag{27}$$

2.2 Solution by Harmonic Differential Quadrature (HDQ) Method

In order to figure out the nonlocal motion equation for the nanoscale rod, Eq. (26), and accordingly to achieve the nonlocal linear axial frequencies for the nanoscale rod, HDQ method was employed. The HDQ method is more impressive compared to the ordinary differential quadrature (DQ) method for solving mechanical problems, especially for vibrating systems, Malekzadeh and Karami (2005), Striz, Wang, and Bert (1995), Bert and Malik (1996). In this method, the partial derivative of a function, with respect to a spatial variable at a given discrete point, approximated by a linear summation of weighted function values at all discrete points chosen in the solution domain of the spatial variable. Assume the amplitude of weighed nanoscale rod is (0 < x < L) and being discretized by N points along x coordinate. If F(x) shows either of deformation function (u) within the nanoscale rod amplitude, or the derivatives of F(x) given that x at the point x_i can be expressed discretely as

$$\frac{d^n F(x_i)}{dx^n}=\sum_{k=1}^{N}A_{ik}^n F(x_k);\qquad n=1,\ldots,N-1 \tag{28}$$

Where A_{ik}^n is the weighting coefficient in conjunction to the n-pth order derivative of $F(x)$, at the discrete point x_i. The description of HDQ method and how to choose the positions of the nodal points utilizing Chebyshev polynomials were presented by Civalek (2004), "Now, the HDQM can be used to discretize the Eq. (26), governing equation, and Eq. (27), boundary condition equation. Before do this, $X=\frac{x}{L}$ and $\bar{U}=\frac{U}{L}$ are used to achieve the non-dimensional form of Eqs. (26) - (27) as bellow

$$\begin{aligned}&\frac{1}{L}\frac{d}{dX}\left(EA\frac{d\bar{U}(X)}{dX}\right)-\frac{1}{L^3}\frac{d^2}{dX^2}\left(\upsilon^2 GI_p\frac{d^2\bar{U}(X)}{dX^2}\right)\\&+\rho A\omega^2 L\bar{U}(X)-\frac{\mu\omega^2}{L}\frac{d^2}{dX^2}\left(\rho A\bar{U}(X)\right)\\&-\frac{1}{L}\frac{d}{dX}\left(\rho\upsilon^2 I_p\omega^2\frac{d\bar{U}(X)}{dX}\right)+\frac{\mu}{L^3}\frac{d^3}{dx^3}\left(\begin{matrix}\rho\upsilon^2 I_p\omega^2\\ *\dfrac{d\bar{U}(X)}{dX}\end{matrix}\right)=0\end{aligned} \tag{29}$$

and,

$$\left[\begin{pmatrix} EA\dfrac{d\bar{U}(X)}{dX}-\dfrac{1}{L^2}\dfrac{d}{dX}\left(v^2GI_p\dfrac{d^2\bar{U}(X)}{dX^2}\right)- \\ \rho v^2I_p\omega^2\dfrac{d\bar{U}(X)}{dX}+\dfrac{\mu}{L^2}\dfrac{d^2}{dX^2}\begin{pmatrix}\rho v^2I_p\omega^2 \\ *\dfrac{d\bar{U}(X)}{dX}\end{pmatrix} \end{pmatrix}_{\delta\bar{U}} + \left(\frac{v^2GI_p}{L}\frac{d^2\bar{U}(X)}{dX^2}\right)_{\delta\bar{U}'}\right]\Bigg|_0^L = 0 \quad (30)$$

Consequently, by performing HDQM, the discretized forms of governing and boundary condition equations at $X_i=\frac{x_i}{L}$ are derived as

$$\begin{aligned} &\frac{1}{L}\sum_{k=1}^{N}\left(A(i,k)EA\sum_{j=1}^{N}\left(A(k,j)\bar{U}(X_j)\right)\right)- \\ &\frac{1}{L^3}\sum_{k=1}^{N}\left(B(i,k)v^2GI_p\sum_{j=1}^{N}\left(B(k,j)\bar{U}(X_j)\right)\right) \\ &+\rho A\omega^2L\bar{U}(X_i)-\frac{\mu\omega^2}{L}\sum_{k=1}^{N}\left(B(i,k)\rho A\bar{U}(X_k)\right) \\ &-\frac{1}{L}\sum_{k=1}^{N}\left(A(i,k)\rho v^2I_p\omega^2\sum_{j=1}^{N}\left(A(k,j)\bar{U}(X_j)\right)\right) \\ &+\frac{\mu}{L^3}\sum_{k=1}^{N}\left(C(i,k)\rho v^2I_p\omega^2\sum_{j=1}^{N}\left(A(k,j)\bar{U}(X_j)\right)\right)=0 \end{aligned} \quad (31)$$

and,

$$\left[\begin{pmatrix} EA\sum_{k=1}^{N}\left(A(i,k)\bar{U}(X_k)\right)- \\ \frac{1}{L^2}\sum_{k=1}^{N}A(i,k)v^2GI_p\sum_{j=1}^{N}\left(B(k,j)\bar{U}(X_j)\right) \\ -\rho v^2I_p\omega^2\sum_{k=1}^{N}\left(A(i,k)\bar{U}(X_k)\right)+ \\ \frac{\mu}{L^2}\sum_{k=1}^{N}\begin{pmatrix}B(i,k)\rho v^2I_p\omega^2* \\ \sum_{j=1}^{N}\left(A(k,j)\bar{U}(X_j)\right)\end{pmatrix} \end{pmatrix}_{\delta\bar{U}(X_i)} + \begin{bmatrix}\left(\frac{v^2GI_p}{L}\sum_{k=1}^{N}\left(B(i,k)\bar{U}(X_k)\right)\right) \\ *\delta\left(\sum_{k=1}^{N}\left(A(i,k)\bar{U}(X_k)\right)\right)\end{bmatrix}\right]\Bigg|_0^L = 0 \quad (32)$$

The discretized forms of BCs, Eq. (32) are employed into the discretized forms of governing equation, Eq. (31), and by separating domain and boundary degrees of freedom (DOF), the following assembled matrix equations are obtained as

$$\begin{bmatrix}[K_{bb}] & [K_{bd}] \\ [K_{db}] & [K_{dd}]\end{bmatrix}\begin{Bmatrix}\{\bar{U}_b\} \\ \{\bar{U}_d\}\end{Bmatrix} = \omega^2\begin{bmatrix}[0] & [0] \\ [M_{db}] & [M_{dd}]\end{bmatrix}\begin{Bmatrix}0 \\ \{\bar{U}_d\}\end{Bmatrix} \quad (33)$$

where $\bar{U}_b$ and $\bar{U}_d$ represent the boundary conditions and amplitude DOF, respectively, as follow

$$\begin{aligned} &\{\bar{U}_b\}=\{\bar{U}(X_1),\bar{U}(X_2),\bar{U}(X_{N-1}),\bar{U}(X_N)\}; \\ &\{\bar{U}_d\}=\{\bar{U}(X_2),\bar{U}(X_3),\dots,\bar{U}(X_{N-3}),\bar{U}(X_{N-2})\} \end{aligned} \quad (34)$$

Some mathematical reductions on Eq. (33) are done, and then the natural linear frequencies of the nanoscale rod can be computed by solving the following equation

$$\begin{aligned} &\left[\left[M_{dd}\right]-\left[M_{db}\right]\left[K_{bb}\right]^{-1}\left[K_{bd}\right]\right]^{-1} \\ &*\left[\left[K_{dd}\right]-\left[K_{db}\right]\left[K_{bb}\right]^{-1}\left[K_{bd}\right]\right]\left\{\bar{U}_d\right\}=\omega^2\left\{\bar{U}_d\right\} \end{aligned} \quad (35)$$

According to the formulations mentioned above and with the help of the MATLAB program solver, a self-developed computer program is written, by which the natural linear frequencies of the nanoscale rod can be extracted.

3. Nonlinear-nonlocal axial free vibrations

3.1 Multi Galerkin method

Eq. (22) is now divided into two dimensions of time and displacement using the Multi Galerkin method as follows

$$u_n(x,t)=\sum_{i=1}^{N}\varphi_i(x)q_i(t) \quad (36)$$

where $q_i(t)$ and $\varphi_i(x)$ are called as the time dependent and the displacement dependent functions, respectively, hence, $q_i(t)$ should be determined and $\varphi_i(x)$ was proposed based on the mode shapes of nanoscale rod vibrations for the clamped-clamped and clamped-free boundary conditions as follow. By replacing Eq. (36) into Eq. (22), putting dimensionless parameters like $X=\frac{x}{L}$; $\bar{\phi}=\frac{\phi}{L}$; $\bar{q}=\frac{q}{q_{Max}}$, and multiplying the achieved result by the function $\bar{\varphi}_m(X)$, and then integrating the governing equation in the range of 0 to 1, we have

$$\begin{aligned} &\ddot{\bar{q}}_m+\xi_1\bar{q}_m+\xi_2\sum_{i=1}^{N}\sum_{j=1}^{N}K_{mij}\bar{q}_i\,\bar{q}_j+ \\ &\xi_3\sum_{i=1}^{N}\sum_{j=1}^{N}\sum_{p=1}^{N}\alpha_{mijp}\,\bar{q}_i\bar{q}_j\bar{q}_p=0 \end{aligned} \quad (37)$$

In the above Eq. (37), the variables are determined as

$$\begin{aligned} &\xi_1=\frac{I_1}{I_2};\xi_2=\frac{q_{Max}}{I_2};\xi_3=\frac{q_{Max}^2}{I_2};\omega_m=\sqrt{\xi_1} \\ &q_{Max}=\text{Nonlinear amplitude};\bar{\phi}=\text{Mode-functions}; \\ &B_2=-\frac{A}{L}Z_1;B_8=\frac{v^2I_pG}{L^3};B_{18}=AL\rho;B_{11}=-\frac{4v^3I_pG}{L^3} \\ &B_{20}=-\left(\frac{v^2I_p\rho}{L}+\frac{\mu A\rho}{L}\right);B_{22}=\frac{\rho\mu v^2I_p}{L^3} \\ &B_4=\left(\frac{4vAZ_4}{L}-\frac{2AZ_2}{L}-\frac{2AZ_1}{L}\right);B_{13}=-\frac{2v^3I_pG}{L^3} \\ &B_6=-\left(\frac{3AZ_2}{L}+\frac{6Av^2Z_4}{L}\right); \end{aligned} \quad (38)$$

$$B_{14}=B_{17}=\frac{v^4 I_p G}{L^3};B_{15}=\frac{4v^4 I_p}{L^3}G$$

$$I_1=\begin{pmatrix}B_2\int_0^1\bar{\phi}_m(X)\frac{d^2\bar{\phi}_i(X)}{dX^2}dX\\+B_8\int_0^1\bar{\phi}_m(X)\frac{d^4\bar{\phi}_i(X)}{dX^4}dX\end{pmatrix}$$

$$I_2=\begin{pmatrix}B_{18}\int_0^1\bar{\phi}_m(X)\bar{\phi}_i(X)dX\\+B_{20}\int_0^1\bar{\phi}_m(X)\frac{d^2\bar{\phi}_i(X)}{dX^2}dX\\+B_{22}\int_0^1\bar{\phi}_m(X)\frac{d^4\bar{\phi}_i(X)}{dX^4}dX\end{pmatrix}$$

$$K_{mij}=\begin{pmatrix}B_4\int_0^1\bar{\phi}_m(X)\frac{d\bar{\phi}_i(X)}{dX}\frac{d^2\bar{\phi}_j(X)}{dX^2}dX+\\B_{11}\int_0^1\bar{\phi}_m(X)\frac{d^2\bar{\phi}_i(X)}{dX^2}\frac{d^3\bar{\phi}_j(X)}{dX^3}dX+\\B_{13}\int_0^1\bar{\phi}_m(X)\frac{d\bar{\phi}_i(X)}{dX}\frac{d^4\bar{\phi}_j(X)}{dX^4}dX\end{pmatrix}$$

$$\alpha_{mijp}=\begin{pmatrix}B_6\int_0^1\bar{\phi}_m(X)\frac{d\bar{\phi}_i(X)}{dX}\frac{d\bar{\phi}_j(X)}{dX}\frac{d^2\bar{\phi}_p(X)}{dX^2}dX\\+B_{14}\int_0^1\bar{\phi}_m(X)\frac{d^2\bar{\phi}_i(X)}{dX^2}\frac{d^2\bar{\phi}_j(X)}{dX^2}\frac{d^2\bar{\phi}_p(X)}{dX^2}dX+\\B_{15}\int_0^1\bar{\phi}_m(X)\frac{d\bar{\phi}_i(X)}{dX}\frac{d^2\bar{\phi}_j(X)}{dX^2}\frac{d^3\bar{\phi}_p(X)}{dX^3}dX+\\B_{17}\int_0^1\bar{\phi}_m(X)\frac{d\bar{\phi}_i(X)}{dX}\frac{d\bar{\phi}_j(X)}{dX}\frac{d^4\bar{\phi}_p(X)}{dX^4}dX\end{pmatrix}$$

3.2 Perturbation analysis

Using the Multiple Scale Method, the nonlinear equations are generally solved with a clear approximation. According to authoritative sources in the field, if the amplitude of the nonlinear vibrations is not too high, this approximation will have an acceptable accuracy. Based on results, to analytically solve the Eq. (37), the nonlinear terms are extended up to$\circ(\varepsilon^3)$ in this way Nayfeh and Nayfeh (1994):

$$\bar{q}_m=\varepsilon\bar{q}_m,\quad \dot{\bar{q}}_m=\varepsilon\dot{\bar{q}}_m,\quad \ddot{\bar{q}}_m=\varepsilon\ddot{\bar{q}}_m \tag{39}$$

To solve the Eq. (40), the Multiple Scale Method (MSM) was utilized. In this method, the time part of the displacement was supposed as an extension of the Minor parameterε. To sort the linear equations estimated by MSM, the parameters of Eq. (40) can be written as

$$\begin{aligned}&\ddot{\bar{q}}_m+\xi_1\bar{q}_m+\varepsilon\xi_2\sum_{i=1}^{N}\sum_{j=1}^{N}K_{mij}\bar{q}_i\bar{q}_j+\\&\varepsilon^2\xi_3\sum_{i=1}^{N}\sum_{j=1}^{N}\sum_{p=1}^{N}\alpha_{mijp}\,\bar{q}_i\bar{q}_j\bar{q}_p=0\end{aligned} \tag{40}$$

According to the MSM, the following independent variables are determined as time scales

$$T_n=\varepsilon^n t \tag{41}$$

The following symbols are used to show derivatives with respect to time scales,

$$\begin{aligned}&D_n=\frac{\partial}{\partial T_n},\quad n=0,1,2,\dots\\&D_0=\frac{\partial}{\partial T_0},\quad D_1=\frac{\partial}{\partial T_1},\quad D_2=\frac{\partial}{\partial T_2}\end{aligned} \tag{42}$$

Similarly, the standard boundary conditions can be also discreted as following:

Therefore, the time derivative can be determined in terms of time scales derivatives

$$\begin{aligned}&\frac{d}{dt}=D_0+\varepsilon D_1+\varepsilon^2 D_2\\&\frac{d^2}{dt^2}={D_0}^2+2\varepsilon D_0D_1+\varepsilon^2\left({D_1}^2+2D_0D_2\right)+\dots\end{aligned} \tag{43}$$

In the perturbation technique, $q(t,\varepsilon)$ is determined up to $\circ(\varepsilon^3)$ as bellow,

$$\begin{aligned}&\bar{q}(t,\varepsilon)=\sum_{n=0}^{2}\varepsilon^n\bar{q}_n(T_0,T_1,T_2)\\&\bar{q}_m(t_i,\varepsilon)=\begin{bmatrix}\bar{q}_{m0}(T_0,T_1,T_2)+\varepsilon\bar{q}_{m1}(T_0,T_1,T_2)\\+\varepsilon^2\bar{q}_{m2}(T_0,T_1,T_2)+\circ\left(\varepsilon^3(t)\right)\end{bmatrix}\end{aligned} \tag{44}$$

The Eqs. (39)-(43) are replaced into the Eq. (40) and balancing the same powers ofε, one achieves

$$\begin{aligned}&\circ(\varepsilon^0):D_0^2\bar{q}_{m0}+\xi_1\bar{q}_{m0}=0\\&\rightarrow D_0^2\bar{q}_{m0}+\omega_m^2\bar{q}_{m0}=0\\&\circ(\varepsilon^1):D_0^2\bar{q}_{m1}+\omega_m^2\bar{q}_{m1}=\begin{bmatrix}-2D_0D_1\bar{q}_{m0}-\\\xi_2\sum_{i=1}^{N}\sum_{j=1}^{N}K_{mij}\,\bar{q}_{i0}\bar{q}_{j0}\end{bmatrix}\\&\circ(\varepsilon^2):D_0^2\bar{q}_{m2}+\omega_m^2\bar{q}_{m2}\\&=\begin{bmatrix}-(D_1^2+2D_0D_2)\bar{q}_{m0}\\-2D_0D_1\bar{q}_{m1}\\-\xi_2\sum_{i=1}^{N}\sum_{j=1}^{N}K_{mij}\left(\bar{q}_{i0}\bar{q}_{j1}+\bar{q}_{i1}\bar{q}_{j0}\right)\\-\xi_3\sum_{i=1}^{N}\sum_{j=1}^{N}\sum_{p=1}^{N}\alpha_{mijp}\,\bar{q}_{i0}\bar{q}_{j0}\bar{q}_{p0}\end{bmatrix}\end{aligned} \tag{45}$$

The Eq. (45) can be simplified as bellow

$$\begin{aligned}&\circ(\varepsilon^0):D_0^2\bar{q}_{m0}+\xi_1\bar{q}_{m0}=0\\&\rightarrow D_0^2\bar{q}_{m0}+\omega_m^2\bar{q}_{m0}=0\\&\circ(\varepsilon^1):D_0^2\bar{q}_{m1}+\omega_m^2\bar{q}_{m1}\\&=-2D_0D_1\bar{q}_{m0}-\xi_2K_{mmm}(\bar{q}_{m0})^2\\&\circ(\varepsilon^2):\\&D_0^2\bar{q}_{m2}+\omega_m^2\bar{q}_{m2}\\&=\begin{pmatrix}-(D_1^2+2D_0D_2)\bar{q}_{m0}-2D_0D_1\bar{q}_{m1}\\-\xi_2\bar{q}_{m0}\left(\sum_{j=1}^{N}\bar{q}_{j1}\left(K_{mmj}+K_{mjm}\right)\right)\\-\xi_3\alpha_{mmmm}(\bar{q}_{m0})^3\end{pmatrix}\end{aligned} \tag{46}$$

And, the first equation of Eq. (46), is solved as bellow

$$\begin{aligned}&\bar{q}_{m0}(T_0,T_1,T_2)=\\&A_m(T_1,T_2)e^{i\omega_mT_0}+\bar{A}_m(T_1,T_2)e^{-i\omega_mT_0}\end{aligned} \tag{47}$$

$A_m(T_1,T_2)$ and $\bar{A}_m(T_1,T_2)$ are the complex functions

in terms of T_1 and T_2 also, i is called as the square root of -1. To make the nonlinear normal mode that reduces to the p^{th} linear mode as ($\varepsilon \to 0$ i.e., the nonlinearity vanishes), we take the solutions of Eq. (46), as follows

$$\begin{matrix} \bar{q}_{p0}(T_0,T_1,T_2) = \\ A_p(T_1,T_2)e^{i\omega_p T_0} + \bar{A}_p(T_1,T_2)e^{-i\omega_p T_0} \to for \quad p \\ \bar{q}_{m0} = 0 \to for \quad m \neq p \end{matrix} \quad (48)$$

The Eq. (48) is replaced into the second equation of Eq. (46) and gives

$$\begin{matrix} D_0^2\bar{q}_{p1} + \omega_p^2\bar{q}_{p1} = \\ \begin{bmatrix} -2D_1\left(A_p i\omega_p e^{i\omega_p T_0} - \bar{A}_p i\omega_p e^{-i\omega_p T_0}\right) \\ -\xi_2 K_{ppp}\left({A_p}^2 e^{2i\omega_p T_0} + 2A_p\bar{A}_p + {\bar{A}_p}^2 e^{-2i\omega_p T_0}\right) \end{bmatrix} \\ D_0^2\bar{q}_{m1} + \omega_m^2\bar{q}_{m1} = \\ -\xi_2 K_{ppp}\left({A_p}^2 e^{2i\omega_p T_0} + 2A_p\bar{A}_p + {\bar{A}_p}^2 e^{-2i\omega_p T_0}\right) \end{matrix} \quad (49)$$

Some secular terms was appeared in the above equation, so, these terms must be vanished Nayfeh and Nayfeh (1994). Because they provide non-periodic responses that are inconvenient with oscillatory suppositions. Eliminating secular terms in Eq. (49) yields

$$\begin{matrix} \frac{\partial A_p}{\partial T_1}, \frac{\partial \bar{A}_p}{\partial T_1} = 0 \to A_p(T_2), \bar{A}_p(T_2) \\ \bar{q}_{p1} = \begin{bmatrix} \frac{\xi_2 K_{ppp}{A_p}^2}{3{\omega_p}^2} e^{2i\omega_p T_0} \\ -\frac{2\xi_2 K_{ppp}A_p\bar{A}_p}{{\omega_p}^2} \end{bmatrix}; for \quad p \\ \bar{q}_{m1} = \begin{bmatrix} \frac{\xi_2 K_{ppp}{A_p}^2}{\left(4{\omega_p}^2 - {\omega_m}^2\right)} e^{2i\omega_p T_0} \\ -\frac{2\xi_2 K_{ppp}A_p\bar{A}_p}{{\omega_m}^2} \end{bmatrix}; for \quad m \neq p \end{matrix} \quad (50)$$

By substituting $\overline{q}_{m0}$, $\bar{q}_{p0}$ and $\overline{q}_{m1}$, $\bar{q}_{p1}$ from Eqs. (48)-(49) into the third equation of Eq. (46) renders

$$\begin{matrix} for \quad p \to D_0^2\bar{q}_{p2} + \omega_p^2\bar{q}_{p2} = \\ \left\{ \begin{bmatrix} -2\frac{\partial A_p}{\partial T_2} i\omega_p + \frac{4\xi_2^2 K_{ppp}^2 {A_p}^2(T_2)\bar{A}_p(T_2)}{{\omega_p}^2} \\ -\frac{2\xi_2^2 K_{ppp}^2 {A_p}^2(T_2)\bar{A}_p(T_2)}{3{\omega_p}^2} \\ -3\xi_3\alpha_{pppp}{A_p}^2(T_2)\bar{A}_p(T_2) \end{bmatrix} e^{i\omega_p T_0} \right. \\ \left. - \left[\frac{2\xi_2^2 K_{ppp}^2 {A_p}^3(T_2)}{3{\omega_p}^2} + \xi_3\alpha_{pppp}{A_p}^3(T_2)\right] e^{3i\omega_p T_0} + cc \right\} \\ for \quad m \neq p \to D_0^2\bar{q}_{m2} + \omega_p^2\bar{q}_{m2} = - \\ \left[\frac{2\xi_2^2 K_{ppp}^2 {A_p}^3(T_2)}{3{\omega_p}^2} + \xi_3\alpha_{pppp}{A_p}^3(T_2)\right] e^{3i\omega_p T_0} + cc \end{matrix} \quad (51)$$

By removing the secular terms of Eq. (51), one renders

$$\begin{bmatrix} -2\frac{\partial A_p}{\partial T_2} i\omega_p + \frac{4\xi_2^2 K_{ppp}^2 {A_p}^2(T_2)\bar{A}_p(T_2)}{{\omega_p}^2} - \\ \frac{2\xi_2^2 K_{ppp}^2 {A_p}^2(T_2)\bar{A}_p(T_2)}{3{\omega_p}^2} - 3\xi_3\alpha_{pppp}{A_p}^2(T_2)\bar{A}_p(T_2) \end{bmatrix} = 0 \quad (52)$$

It is supposed that, $A_p(T_2)$ function can be determined as

$$\begin{matrix} \underbrace{A_p(T_2)}_{\text{complex function}} = \frac{1}{2}ae^{i\beta} \to a, \beta \\ \text{are real functions of } T_2; \\ So, \quad A_p(T_2) = \frac{1}{2}a(T_2)e^{i\beta(T_2)} \end{matrix} \quad (53)$$

By replacing Eq. (53) into the Eq. (52) gives

$$\begin{matrix} \begin{bmatrix} -ia'\omega_p + a\beta'\omega_p + \frac{\xi_2^2 K_{ppp}^2 a^3}{2\omega_p^2} \\ -\frac{\xi_2^2 K_{ppp}^2 a^3}{12\omega_p^2} - \frac{3}{8}\xi_3\alpha_{pppp}a^3 \end{bmatrix} = 0 \\ \to \left\{ \begin{matrix} \text{Real part} = 0 \\ \text{Imaginary part} = 0 \end{matrix} \right\} \\ \left\{ \begin{matrix} a\beta'\omega_p + \frac{5\xi_2^2 K_{ppp}^2 a^3}{12\omega_p^2} - \frac{3}{8}\xi_3\alpha_{pppp}a^3 = 0 \\ -a'\omega_p = 0 \end{matrix} \right\} \\ \to \left\{ \begin{matrix} \beta' = -\frac{5\xi_2^2 K_{ppp}^2 a^2}{12\omega_p^3} + \frac{3}{8\omega_p}\xi_3\alpha_{pppp}a^2 \\ a' = 0 \end{matrix} \right\} \\ \left\{ \begin{matrix} \frac{d\beta}{dT_2} = -\frac{5\xi_2^2 K_{ppp}^2 a^2}{12\omega_p^3} + \frac{3}{8\omega_p}\xi_3\alpha_{pppp}a^2 \\ \frac{da}{dT_2} = 0 \end{matrix} \right\} \\ \to \left\{ \begin{matrix} \beta(T_2) = \left(-\frac{5\xi_2^2 K_{ppp}^2 a^2}{12\omega_p^3} + \frac{3}{8\omega_p}\xi_3\alpha_{pppp}a^2\right)T_2 + \beta_0 \\ a(T_2) = a = \text{constant} \end{matrix} \right\} \\ finally \to A_p(T_2) = \frac{1}{2}ae^{i\left(\left(\frac{3}{8\omega_p}\xi_3\alpha_{pppp}a^2 - \frac{5\xi_2^2 K_{ppp}^2 a^2}{12\omega_p^3}\right)T_2 + \beta_0\right)} \end{matrix} \quad (54)$$

And to solve the third section of Eq. (46) can be written as

$$\begin{matrix} for \quad p \to \bar{q}_{p2}(T_0,T_1,T_2) = \\ \left(\frac{\xi_2^2 K_{ppp}^2 {A_p}^3}{12\omega_p^4} + \frac{\xi_3\alpha_{pppp}{A_p}^3}{8\omega_p^2}\right) e^{3i\omega_p T_0} \\ for \quad m \neq p \to \bar{q}_{m2}(T_0,T_1,T_2) = \\ \left(\frac{2\xi_2^2 K_{ppp}^2 {A_p}^3}{3\omega_p^2} + \xi_3\alpha_{pppp}{A_p}^3\right)\frac{e^{3i\omega_p T_0}}{9\omega_p^2 - \omega_m^2} \end{matrix} \quad (55)$$

And, the end of the general answer was written in the form of Eq. (56).

Now, the Eq. (54) into the Eq. (48) was putted, consequently, the nonlinear nonlocal frequencies for the nanoscale rods are derived as Eq. (57).

Eq. (56) indicates that there are three cases in which the relationships of internal resonances occur, (one to-one$(\omega_p = \omega_m)$, two-to-one$(2\omega_p = \omega_m)$, and three-to-one $(3\omega_p = \omega_m)$internal resonances).

4. Verify study

The gold nanorod model was developed to study various types of axisymmetric beam theories in the presence of internal modal interactions based on nonlocal continuum theory, which has already proven to be a very reliable tool

for mathematical modeling. Since the gold nanorod model has not yet been investigated by experimental methods and MD simulation in mechanical sciences, this research can be a starting point in the theoretical studies of dynamic vibrational behavior of nanostructures under the influence of internal resonances with some other physical effects. However, to some extent, experimental studies have been carried out on the optimized synthesis of gold nanorods, which are more important in the field of medicine and treatment of diseases. The main goal in the synthesis of gold nanorods has been to achieve the optimal dimensions with the highest internal resonances. According to the above studies, it can be concluded that: i) In order to achieve the long shelf life of gold nanorods in the living circulatory system, the particle size must be less than 100 nanometers (Choi *et al*. 2010). ii) Synthesized gold nanorods with dimensions of 12 nm (wide) by 37 nm (length) have a maximum Plasmon absorption wavelength of about 800 nm, (Pitsillides *et al*. 2003). In order to better understand the mentioned items, pay attention to Figs. 2(a) - 2(b).

$$\bar{q}_p(t,\varepsilon) = \bar{q}_{p0} + \varepsilon\bar{q}_{p1} + \varepsilon^2\bar{q}_{p2}$$
$$\bar{q}_p(t,\varepsilon) = \left(\begin{array}{l} A_p e^{i\omega_p T_0} + \bar{A}_p e^{-i\omega_p T_0} + \\ \varepsilon\left(\frac{\xi_2 K_{ppp} {A_p}^2}{3{\omega_p}^2} e^{2i\omega_p T_0} - \frac{2\xi_2 K_{ppp} A_p \bar{A}_p}{{\omega_p}^2}\right) \\ +\varepsilon^2\left(\left(\frac{\xi_2^2 K_{ppp}^2 {A_p}^3}{12\omega_p^4} + \frac{\xi_3 \alpha_{pppp} {A_p}^3}{8\omega_p^2}\right) e^{3i\omega_p T_0}\right) + O(\varepsilon^3) \end{array}\right)$$
$$\bar{q}_m(t,\varepsilon) = \bar{q}_{m0} + \varepsilon\bar{q}_{m1} + \varepsilon^2\bar{q}_{m2} \quad (56)$$
$$\bar{q}_m(t,\varepsilon) = \left(\begin{array}{l} \varepsilon\left(\frac{\xi_2 K_{ppp} {A_p}^2}{(4{\omega_p}^2 - {\omega_m}^2)} e^{2i\omega_p T_0} - \frac{2\xi_2 K_{ppp} A_p \bar{A}_p}{{\omega_m}^2}\right) + \\ \varepsilon^2\left(\begin{array}{l} \left(\frac{2\xi_2^2 K_{ppp}^2 {A_p}^3}{3\omega_p^2} + \xi_3 \alpha_{pppp} {A_p}^3\right) \\ * \frac{e^{3i\omega_p T_0}}{9\omega_p^2 - \omega_m^2} \end{array}\right) \\ +O(\varepsilon^3) \end{array}\right)$$

$$\bar{q}_{p0} = a_p\, Cos\left[t\left(\left(\frac{3\xi_{\ 3}\alpha_{pppp} a_p^2}{8\omega_p} - \frac{5\xi_2^2 K_{ppp}^2 a_p^2}{12\omega_p^3}\right)\varepsilon^2 + \omega_p\right) + \beta_0\right] \quad (57)$$
$$\omega_{\text{Non-Linear}}^{non-local}\big|_p = \left(\frac{3\xi_{\ 3}\alpha_{pppp} a_p^2}{8\omega_p} - \frac{5\xi_2^2 K_{ppp}^2 a_p^2}{12\omega_p^3}\right)\varepsilon^2 + \omega_p$$
$$\Rightarrow a_p = \frac{1}{\varepsilon} \rightarrow \omega_{\text{Non-Linear}}^{non-local}\big|_p = \left(\frac{3\xi_{\ 3}\alpha_{pppp}}{8\omega_p} - \frac{5\xi_2^2 K_{ppp}^2}{12\omega_p^3}\right) + \omega_p$$

After finding out the optimal dimensions based on the experimental synthesis of gold nanorods, now we validate the theoretical solution of the problem by comparing it with the existing literature. Two comparative study were done to show the correctness of the derived equations. For this purpose, first, the natural frequencies of this research were compared to those reported in the literature (Fernandes *et al*. 2017), without considering the effect of the nonlocal parameter. In the mentioned reference the linear and nonlinear free axial vibration of a single walled carbon nanotube embedded in an elastic medium were evaluated,

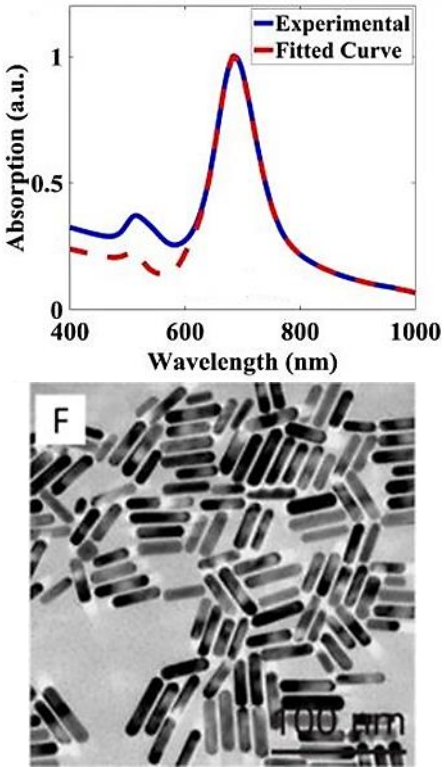

Fig. 2 (a) The absorption spectrum of the synthesized gold nanoscale rods is observed, which has the highest light absorption at 808 nm, (Kumar *et al*. 2019) (b) 50 nm micrographs of the synthesized gold nanoscale rods were prepared under the microscope, (An *et al*. 2017)

using the strain and velocity gradient theory. Non-dimensional linear and nonlinear frequencies (for clamped-clamped and clamped-free boundary conditions) of nanorod were shown in Table 1. Table 1 demonstrates that the results of the classic study are the same as those reported by (Fernandes *et al*. 2017). It can imply the accuracy of presented formulations and results in local model.

Next, to confirm the accuracy of the extracted formulations and methods for the nonlocal model, the results of the present study, which were calculated by MS method, were compared to the results of the research, Civalek and Numanoğlu (2020), which were obtained using the finite element numerical method. The results in Table 2 show a good compliance, which is based on the correctness of the method used in the current paper.

5. Discussion

Many studies on gold nanorods are being done every day by experts in physics, chemistry, nanomedicine, and nano-biotechnology sciences. According to them, attractive results have been achieved in the use of gold nanorods in the treatment of diseases such as cancer. Physics of gold nanoparticles: one of the most important properties of metal nanoparticles is their plasmonic properties Kik and Brongersma (2007). Plasma frequency occurs in most metals in the ultraviolet region. But in some, such as copper

Table 1 Comparison of the first three non-dimensional natural axial frequencies of local model

Type of BCs		n_1		n_2		n_3	
		ω linear	ω nonlinear	ω linear	ω nonlinear	ω linear	ω nonlinear
Clamped-Clamped	(Fernandes *et al*. 2017)	3.1416	3.1852	6.2832	6.6320	9.4248	10.6020
	Present study	3.1416	3.1852	6.2832	6.6320	9.4248	10.6020
Clamped-Free	(Fernandes *et al*. 2017)	1.5708	1.5501	4.7124	4.7810	7.8540	8.4044
	Present study	1.5708	1.5501	4.7124	4.7810	7.8540	8.4044

Table 2 Comparison of the first three non-dimensional natural axial frequencies of nonlocal model

Present work (analytical method)				
Boundary Conditions	Clamped-clamped BCs		Clamped-free BCs	
Mode number	μ=0.2	μ=0.3	μ=0.2	μ=0.3
n = 1	2.67	2.28	1.49	1.42
n = 2	3.92	2.95	3.43	2.73
n = 3	4.42	3.15	4.22	3.07
Civalek and Numanoğlu (2020), (numerical method)				
n = 1	2.6601	2.2862	1.4986	1.4209
n = 2	3.9124	2.9446	3.4293	2.7213
n = 3	4.4169	3.1426	4.2178	3.0684

and gold, due to electron band transitions, it is in the visible spectrum region, creating a strong absorption spectrum in this region. Since visible light radiation does not damage the body tissue, the plasmonic property of gold nano-particles is used in medical applications (He *et al*. 2005). With recent advances in chemistry, it is possible to implement color nanostructures with plasmonic properties in terms of various shapes such as spheres, triangles, prisms, rods and cubes. By changing the geometry of the surface, the density of the electric field changes, which changes the vibrational frequency of the electrons. Therefore, particles with different shapes and sizes show different plasmonic properties. As a result, by controlling the shape and size, the peak of surface Plasmon resonance can be changed in the visible to near-infrared range Sun and Xia (2003). Research has shown that by transforming gold nanoparticles from other shapes into rods, the oscillation frequency range of the surface Plasmon (Surface Plasmon Resonance: SPR) of the nanoparticles changes Arvizo, Bhattacharya, and Mukherjee (2010). Scientists have used these properties of gold nanorods to target and reduce the size of tumors. Chemistry of gold nanoparticles: The choice of nanoparticle synthesis method is very important; because the physical and chemical properties of the particles depend on it, and according to the type of coating agent, the need for stabilizer and the desired size is selected Louis and Pluchery (2012).

According to the above studies, it can be concluded that: i) In order to achieve the long shelf life of gold nanorods in the living circulatory system, the particle size must be less than 100 nanometers. ii) Synthesized gold nanorods with dimensions of 12 nm (wide) by 37 nm (length) have a maximum Plasmon absorption wavelength of about 800 nm.

The contents mentioned in the previous paragraphs are the study of the properties of gold nanorods based on the sciences of physics, chemistry and nanomedicine without considering the mechanical and vibrational properties of gold nanorods. Likely, considering the properties of gold nanorods is also very important from the point of view of mechanical engineering, and by recognizing them, it can be used to synthesize useful gold nanorods in order to better treat diseases. Hence, in this research, all the mechanical and vibrational properties of gold nanorods have been carefully investigated in a targeted manner for their applied dimensions in the medical sciences.

5.1 Comparison study of all three axial beams theories

In this section, a comparative study was conducted in terms of linear and nonlinear frequency changes for both local and nonlocal models based on the aspect ratio of gold nanorods for the number of first and third frequencies, considering all three simple, Rayleigh and Bishop theories. To this end, a gold nanorod was considered with an aspect ratio of $3 \leq \frac{L}{d_o} \leq 10$, nonlinear amplitudes $0 \leq q_{max}$ and nonlocal coefficients $0 \leq \mu \leq 0.5$. As illustrated in Fig. 3, as the gold nanorods become thinner, the results of linear and nonlinear frequencies match for all three Simple, Rayleigh and Bishop axial beams theories. In other words, the effects of inertial and shear can be neglected by thinning gold nanorods. It is noteworthy that the results of the three theories have a lot of adaptation in the first frequency mode, but this adaptation decreases in higher modes. It means that the effects of inertial and shear that show the difference between theories are superior in higher modes and the importance of using different theories in higher modes is

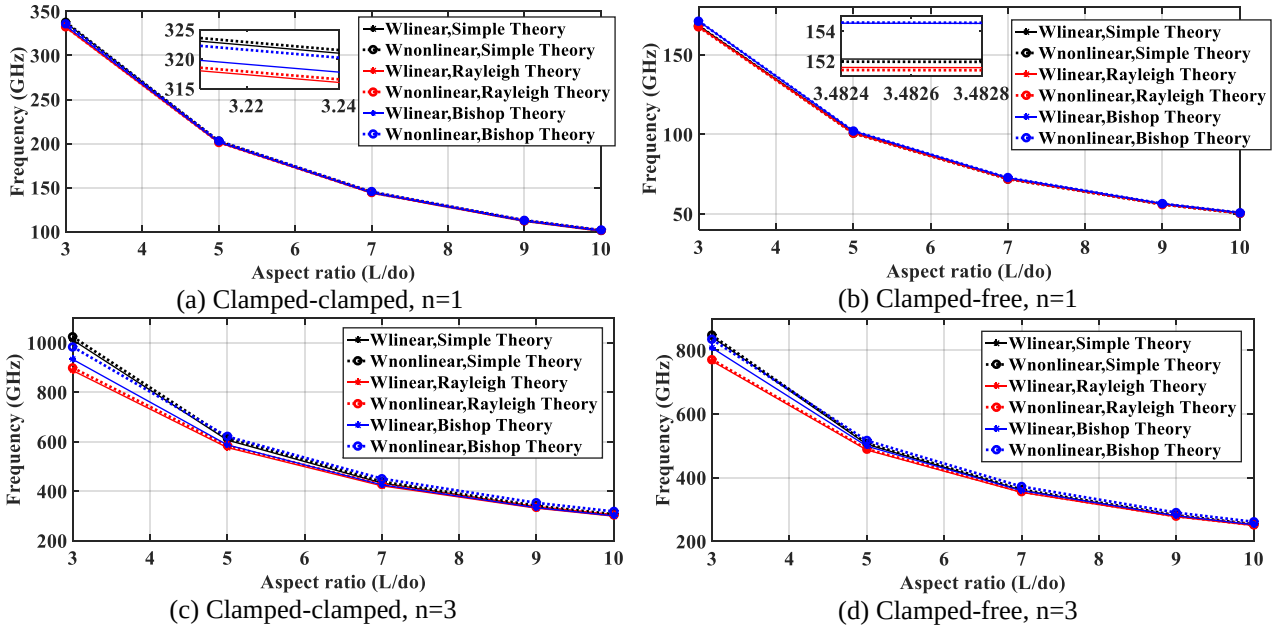

(a) Clamped-clamped, n=1 (b) Clamped-free, n=1

(c) Clamped-clamped, n=3 (d) Clamped-free, n=3

Fig. 3 Variations of linear and nonlinear frequencies versus aspect ratio of gold nanorod in terms of Simple (without inertial and shear effects), Rayleigh (with inertial and without shear effects) and Bishop (with inertial and shear effects) axial beams theories for local case ($\mu = 0$), by considering $q_{max} = 0.1$

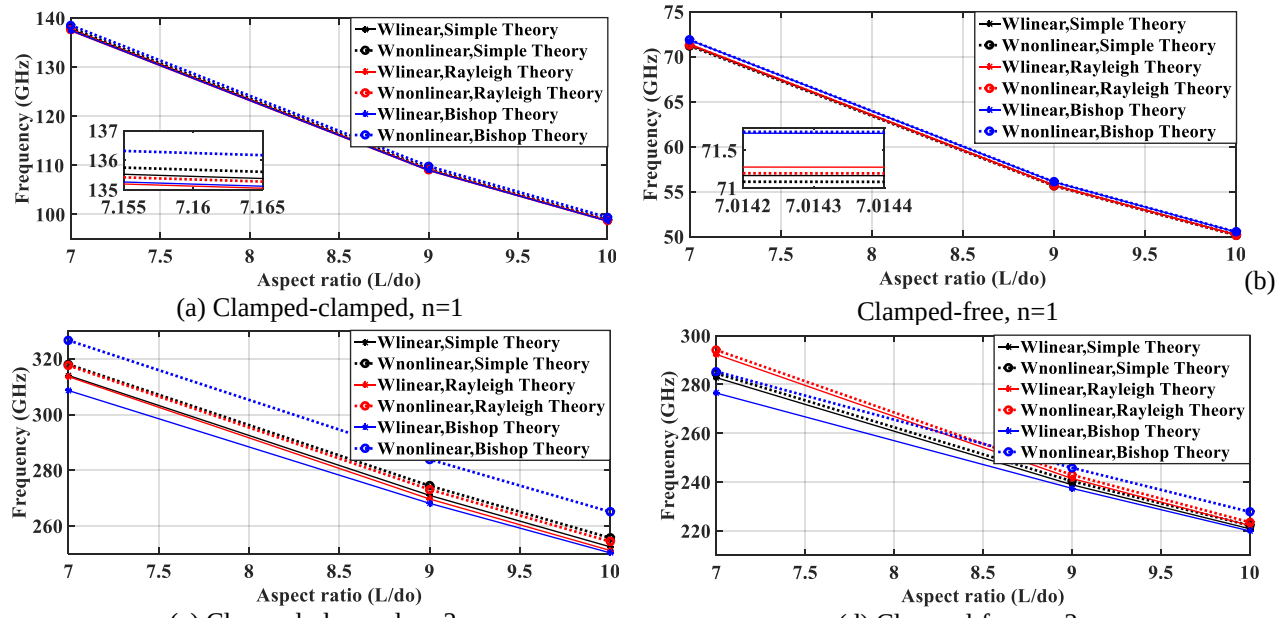

(a) Clamped-clamped, n=1 (b) Clamped-free, n=1

(c) Clamped-clamped, n=3 (d) Clamped-free, n=3

Fig. 4 Variations of linear and nonlinear frequencies versus aspect ratio of gold nanorod in terms of Simple (without inertial and shear effects), Rayleigh (with inertial and without shear effects) and Bishop (with inertial and shear effects) axial beams theories for nonlocal case ($\mu = 0.5$ (nm^2)), by considering $q_{max} = 0.1$

more obvious. Figs. 3(a) and 3(c) show the variations of local linear and nonlinear frequencies for the first and third modes, respectively, in clamped-clamped boundary conditions. Figs. 3(b) and 3(d) also indicate the same changes for clamped-free boundary conditions that the trend of frequency changes is the same for both boundary conditions.

Considering the effects of the nonlocal factor on the values of linear and nonlinear frequencies in Fig. 4, the variations of linear and nonlinear nonlocal frequencies are also plotted for all three theories and clamped-clamped and clamped-free boundary conditions. In order to better show the difference between the theories, the aspect ratio of gold nanorods was considered equal to $7 \leq \frac{L}{d_o} \leq 10$. The differences in theories are more pronounced in thick nanorods, which indicates that the theory used varies depending on the thickness of the nanorods. Figs. 4(a)-(d) show the changes of linear and nonlinear frequencies in terms of nonlocal case versus aspect ratio of gold nanoscale

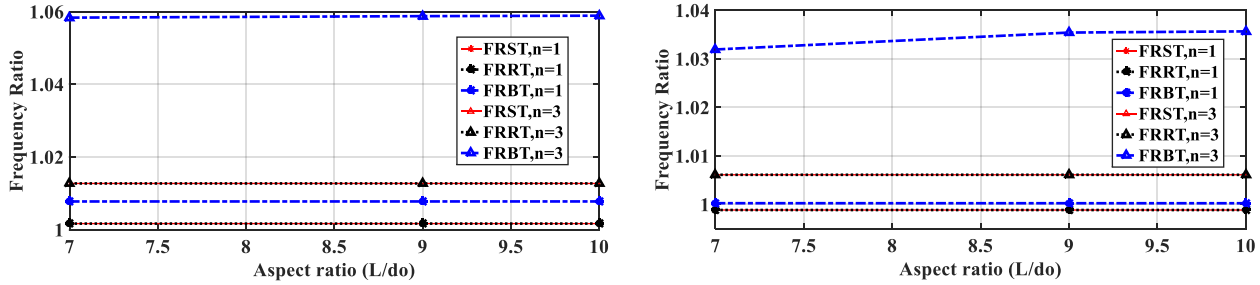

(a) Clamped-clamped (b) Clamped-free

Fig. 5 Variations of frequency ratios versus aspect ratio of gold nanoscale rod based on nonlinear factor for FRST (Simple theory), FRRT (Rayleigh Theory) and FRBT (Bishop Theory) in terms of first and third frequency modes by considering

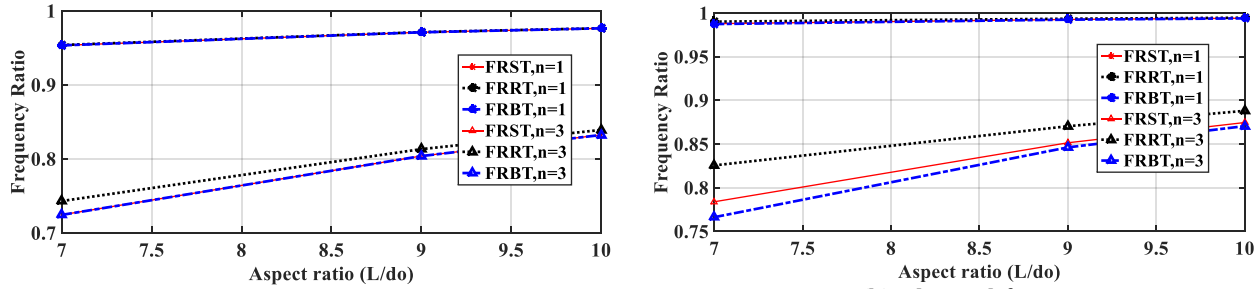

(a) Clamped-clamped (b) Clamped-free

Fig. 6 Variations of frequency ratios versus aspect ratio of gold nanoscale rod based on nonlocal factor for FRST (Simple theory), FRRT (Rayleigh Theory) and FRBT (Bishop Theory) in terms of first and third frequency modes by considering

rod for the first and third modes, respectively, considering clamped-clamped and clamped-free boundary conditions.

Figs. 3 and 4 display the importance of correctly selecting the axial beam theories by considering the thickness of the gold nanorod and the number of frequency modes. Another important factor studied in this research include the effects of nonlocal and nonlinear factors on all three Simple, Rayleigh and Bishop axial beams theories. To better illustrate the effects of nonlocal and nonlinear factors on all three Simple, Rayleigh, and Bishop theories, frequency ratios of FRST, FRRT, and FRBT are defined according to Eq. 58, respectively.

Simple Theory ⇒

$$FRST = \frac{\omega_{Nonlocal-Nonlinear}}{\omega_{Nonlocal-Linear}}\Big|_{Nonlinear\ \ effects} ; \frac{\omega_{Nonlocal-Nonlinear}}{\omega_{Local-Nonlinear}}\Big|_{Nonlocal\ \ effects}$$

Rayleigh Theory ⇒

$$FRRT = \frac{\omega_{Nonlocal-Nonlinear}}{\omega_{Nonlocal-Linear}}\Big|_{Nonlinear\ \ effects} ; \frac{\omega_{Nonlocal-Nonlinear}}{\omega_{Local-Nonlinear}}\Big|_{Nonlocal\ \ effects} \quad (58)$$

Bishop Theory ⇒

$$FRBT = \frac{\omega_{Nonlocal-Nonlinear}}{\omega_{Nonlocal-Linear}}\Big|_{Nonlinear\ \ effects} ; \frac{\omega_{Nonlocal-Nonlinear}}{\omega_{Local-Nonlinear}}\Big|_{Nonlocal\ \ effects}$$

Figs. 5(a) and 5(b) show a comparison between various axial beams theories in terms of investigating the effects of nonlinear factor for a gold nanorod. As it is known, the effects of nonlinear factor for both Simple and Rayleigh theories with the considered aspect ratio of gold nanorod are the same for the first and third frequency modes, while the effects of nonlinear factor in the first frequency mode are insignificant for both Simple and Rayleigh theories. The nonlinear effects of third frequency mode more increases nonlocal frequency values. For Bishop Theory, both in the first frequency mode and in the third frequency mode, nonlinear effects increase the values of non-local frequencies. In other words, in higher modes, nonlinear effects are more observed in all three theories. The trend of the effects of nonlinear factor on frequency variations is the same for both clamped-clamped and clamped-free boundary conditions, with the difference that in clamped-clamped boundary conditions we see higher values for nonlocal frequencies (see Figs. 5(a) and 5(b)).

Finally, in Figs. 6(a) and 6(b), the effects of nonlocal factor on three different axial beams theories were evaluated for both clamped-clamped and clamped-free boundary conditions, respectively. As shown in Fig. 6, the effects of nonlocal factor are the same for all three theories in the first frequency mode, but for the third frequency mode (higher frequency modes) its effects reduce the values of the nonlinear frequencies. Of course, in the clamped-clamped boundary conditions, the decreasing effects of the nonlocal factor are greater for Simple and Bishop theories than for the Rayleigh theory. And, in clamped-free boundary

Table 3 List of internal resonances for extracting accurate nonlinear amplitudes considering Simple Theory

m	p	$\omega_m = 2\omega_p$				$\omega_m = 3\omega_p$			
		L/do=7 (Aspect ratio of gold nanorod)		L/do=9		L/do=7		L/do=9	
		q_{max} (Nonlinear amplitude)		q_{max}		q_{max}		q_{max}	
		$\mu = 0$	$\mu = 0.5_{(nm^2)}$	$\mu = 0$	$\mu = 0.5_{(nm^2)}$	$\mu = 0$	$\mu = 0.5_{(nm^2)}$	$\mu = 0$	$\mu = 0.5_{(nm^2)}$
2	1	non	0.563761	non	0.447339	1.205637	1.491179	1.205637	1.389239
3	1	non	non	non	non	non	0.547966	non	0.440859
3	2	0.833163	1.260145	0.833163	1.120240	3.437286	non	3.437286	non
4	3	1.314082	non	1.314082	4.023144	non	non	non	non
4	2	0	0.512542	0	0.423692	0.618626	1.032219	0.618626	0.909951
5	3	0.329580	0.697672	0.329580	0.612146	0.861285	2.365321	0.861285	1.706589
4	1	non	non	non	non	non	0.278259	non	0.107094
5	2	non	0.319426	non	0.227663	0.274473	0.634050	0.274473	0.549036
5	1	non	non	non	non	non	0.150921	non	non
Clamped-free boundary conditions									
2	1	non	non	non	non	0.001230	0.608199	0.001230	0.483343
3	2	0.660977	0.938471	0.660977	0.853390	1.447961	1.759998	1.447961	1.656454
4	3	0.962771	1.464012	0.962771	1.308822	non	non	non	non
4	2	non	0.362670	non	0.227061	0.494006	0.811920	0.494006	0.723690
5	4	1.596927	non	1.596927	non	non	non	non	non
5	3	0.262294	0.614867	0.262294	0.537043	0.722798	1.187423	0.722798	1.057871
5	2	non	0.150295	non	non	0.001348	0.523280	0.001348	0.435319

Table 4 List of relationships of internal modals interactions in terms of Rayleigh's and Bishop's theories by considering L/do = 7

Clamped-clamped BCs.							
Rayleigh Theory				Bishop Theory			
$\omega_m = 2\omega_p$		$\omega_m = 3\omega_p$		$\omega_m = 2\omega_p$		$\omega_m = 3\omega_p$	
$\mu = 0$	$\mu = 0.5_{(nm^2)}$	$\mu = 0$	$\mu = 0.5_{(nm^2)}$	$\mu = 0$	$\mu = 0.5_{(nm^2)}$	$\mu = 0$	$\mu = 0.5_{(nm^2)}$
$\omega_3 = 1.97\omega_2$	$\omega_2 = 1.99\omega_1$	$\omega_2 = 2.97\omega_1$	$\omega_2 = 2.99\omega_1$	$\omega_3 = 2.58\omega_2$	$\omega_2 = 2.64\omega_1$	$\omega_2 = 4.67\omega_1$	$\omega_2 = 4.6\omega_1$
$\omega_4 = 1.96\omega_3$	$\omega_3 = 2\omega_2$	$\omega_3 = 2.95\omega_2$	$\omega_4 = 3.05\omega_2$	$\omega_4 = 2.16\omega_3$	$\omega_3 = 2.43\omega_2$	$\omega_3 = 3.1\omega_2$	$\omega_4 = 4.26\omega_2$
$\omega_4 = 1.93\omega_2$	$\omega_4 = 2.03\omega_2$	$\omega_4 = 2.9\omega_2$	$\omega_5 = 3.1\omega_3$	$\omega_4 = 1.95\omega_2$	$\omega_4 = 3.03\omega_2$	$\omega_4 = 4.58\omega_2$	$\omega_5 = 2.98\omega_3$
$\omega_5 = 1.91\omega_3$	$\omega_5 = 2.07\omega_3$	$\omega_5 = 2.87\omega_3$	$\omega_4 = 3.04\omega_1$	$\omega_5 = 2.6\omega_3$	$\omega_5 = 2.56\omega_3$	$\omega_5 = 3.68\omega_3$	$\omega_4 = 4.23\omega_1$
Clamped-free BCs.							
$\omega_3 = 1.97\omega_2$	$\omega_3 = 2.04\omega_2$	$\omega_2 = 2.98\omega_1$	$\omega_2 = 3.03\omega_1$	$\omega_3 = 2.75\omega_2$	$\omega_3 = 2.6\omega_2$	$\omega_2 = 2.98\omega_1$	$\omega_2 = 3.9\omega_1$
$\omega_4 = 1.96\omega_3$	$\omega_4 = 2.05\omega_3$	$\omega_3 = 2.96\omega_2$	$\omega_4 = 3.14\omega_2$	$\omega_4 = 2.4\omega_3$	$\omega_4 = 2.48\omega_3$	$\omega_3 = 3.93\omega_2$	$\omega_4 = 5.35\omega_2$
$\omega_5 = 1.95\omega_4$	$\omega_4 = 2.09\omega_2$	$\omega_4 = 2.91\omega_2$	$\omega_5 = 3.45\omega_3$	$\omega_5 = 2.02\omega_4$	$\omega_4 = 2.81\omega_2$	$\omega_4 = 4.76\omega_2$	$\omega_5 = 7.27\omega_3$
$\omega_5 = 1.92\omega_3$	$\omega_5 = 2.22\omega_3$	$\omega_5 = 2.88\omega_3$	$\omega_5 = 3.36\omega_2$	$\omega_5 = 2.51\omega_3$	$\omega_5 = 5.29\omega_3$	$\omega_5 = 4.25\omega_3$	$\omega_5 = 9.36\omega_2$

conditions, the decreasing effects of the nonlocal factor are greater for the Bishop's theory than for the Simple theory and the Simple theory more than for the Rayleigh theory in the third frequency mode, respectively.

5.2 Analysis of internal modals interactions

As one of important characteristics of the nonlinear system containing the geometric nonlinearity, the internal resonance between the system's modes may occur and affect the nonlinear properties of the system. In this paper, first, the internal resonance conditions of the gold nanoscale rod were investigated by considering inertial and shear effects based on the method of multiple scales. Next, the effects of different theories of axial nonlinear beams containing Simple, Rayleigh and Bishop theories on the relationship of internal resonances were studied in detail. Hence, the internal resonance relations for the first five frequency modes were evaluated. Also, in order to better show the effects of different theories on the relationships of internal

modals interactions for gold nanorods, first the characteristics of the vibration system in which the state of internal resonances occur were extracted based on the Simple theory. Then, using these extracted characteristics of gold nanorods, considering the Rayleigh and Bishop theories, the relationships of internal resonances have been recalculated. The results show that the theory used significantly affects the relationships of internal resonances, so depending on the thickness of the gold nanorod, it is important to decide which theory to use. In other words, the effects of inertia and shear, which were considered in Rayleigh's and Bishop's theories, respectively, have a profound effect on the relationships of internal modals interactions, which were more observed in higher frequency modes. Tables 3 and 4 have been prepared for this purpose.

According to Table 3, the exact nonlinear amplitudes of gold nanorods in which internal resonances are generated and computed based on Simple theory. Now that these are all the properties of gold nanorods, the relationships of internal modals interactions of gold nanorods are being rediscovered based on Rayleigh's and Bishop's theories. This study shows the importance of the choice of theories and their effects on the internal resonance ratios of gold nanorods. Table 4 is provided for this purpose. As previously calculated, in the vibration problem of gold nanorods studied in this research, the internal resonance ratios as $2\omega_p = \omega_m$, and $3\omega_p = \omega_m$ for two general modes p and m have been extracted. So that if these ratios are shifted, no more internal resonances will occur. Table 4 shows that the variations in these internal resonance's ratios are due to changes in theories. This suggests that different theories have a profound effect on internal resonances ratios. As a result, depending on the type of investigation required and the thickness of the gold nanorod, a suitable theory should be identified and based on that hypothesis, the exact nonlinear amplitudes of the occurrence of internal resonances should be derived. The presence of internal resonances in nonlinear systems is very important, which is why this issue has been addressed in this study.

6. Conclusions

The vibrational behavior of gold nanorods was studied to extract the internal modal interactions caused by nonlocal effects. The presented gold nanorod mechanical model is based on Bishop's theory in mechanics. Accordingly, the nonlinear governing equations of a nonlinear structure were obtained by applying the nonlocal elasticity theory. The system of partial differential equations was solved linearly and nonlinearly by HDQ and MS methods, respectively. The important conclusions can be categorized as follows:

• It is proved that the occurrence of internal resonance depends on the type of theories, which is important for extracting the accurate nonlinear domain of gold nanoscale rod.

• The results show that the inertial effects alone have less effect on disturbing the internal resonances ratios of gold nanoscale rod than its effects in the presence of simultaneous shear effects.

• The presented theoretical model has the ability to predict very suitable results for extracting the internal modal interactions in the gold nanorod.

• As the nonlocal parameter of the gold nanorod increases, the maximum nonlinear amplitude occurs.

• Shear and inertial analysis have a significant effect on internal modal interactions in gold nanorods.

• By adding nonlocal effects in a gold nanorod, the internal modal interactions resulting from the unique structure can be enhanced.

In general, gold nanorods with unique structure and useful properties can be synthesized to have the best performance in terms of dimensions and internal resonances in the treatment, which has been comprehensively studied in this research for a unique structure.

Conflict of interest

The authors declare that they have no conflict of interest,

References

Amabili, M. (2018), "Nonlinear damping in large-amplitude vibrations: modelling and experiments", *Nonlinear Dyn.*, **93**(1), 5-18, https://doi.org/10.1007/s11071-017-3889-z

Abadeer, N.S. and Catherine J.M. (2016), "Recent progress in cancer thermal therapy using gold nanoparticles", *J. Phys. Chem.*, **120**(9), 4691-716. https://doi.org/10.1021/acs.jpcc.5b11232

Arvizo, R., Resham B. and Priyabrata M. (2010), "Gold nanoparticles: opportunities and challenges in nanomedicine", *Expert Opin. Drug Discover.*, **7**, 753-763. https://doi.org/10.1517/17425241003777010

Aydogdu, M. (2009), "Axial vibration of the nanorods with the nonlocal continuum rod model", *Physica E*, **41**, 861-64. https://doi.org/10.1016/j.physe.2009.01.007

Aydogdu, M. (2015), "A nonlocal rod model for axial vibration of double-walled carbon nanotubes including axial van der Waals force effects", *J. Vib. Control*, **21**, 3132-54. https://doi.org/10.1177/1077546313518954

An, L., Wang, Y., Tian, Q. and Yang, S. (2017), "Small gold nanorods: recent advances in synthesis, biological imaging, and cancer therapy", *Materials*, **10**(12), 1372. https://doi.org/10.3390/ma10121372

Bert, C.W. and Moinuddin, M. (1996), "Differential quadrature method in computational mechanics: A review", *Appl. Mech. Rev. Jan*, **49**(1), 1-28. https://doi.org/10.1115/1.3101882

Bacigalupo, A. and Gambarotta, L. (2019). Generalized micropolar continualization of 1D beam lattices. *Int. J. Mech. Sci*, **155**, 554-570. https://doi.org/10.1016/j.ijmecsci.2019.02.018

Bacigalupo, A. and Gambarotta, L. (2021), "Identification of non-local continua for lattice-like materials", *Int. J. Eng. Sci.*, **159**, 103430. https://doi.org/10.1016/j.ijengsci.2020.103430

Civalek, Ö. (2004), "Application of differential quadrature (DQ) and harmonic differential quadrature (HDQ) for buckling analysis of thin isotropic plates and elastic columns", *Eng. Struct.* **26**, 171-186. https://doi.org/10.1016/j.engstruct.2003.09.005

Choi, H.S., Liu, W., Liu, F., Nasr, K., Misra, P., Bawendi, M.G. and Frangioni, J.V. (2010), "Design considerations for tumour-targeted nanoparticles", *Nat. Nanotechnol*, **5**(1), 42-47. https://doi.org/10.1038/nnano.2009.314

Civalek, Ö. and Numanoğlu, H.M. (2020), "Nonlocal finite element analysis for axial vibration of embedded love–bishop nanorods", *Int. J. Mech. Sci.*, **188**, 105939, https://doi.org/10.1016/j.ijmecsci.2020.105939

Eltaher, M.A, Khater, M.E, and Samir A.E. (2016), "A review on nonlocal elastic models for bending, buckling, vibrations, and wave propagation of nanoscale beams", *Appl. Math. Modell*, **40**, 4109-4128. https://doi.org/10.1016/j.apm.2015.11.026

Eringen, A.C. (1983), "On differential equations of nonlocal elasticity and solutions of screw dislocation and surface waves", *J. Appl. Phys.*, **54**, 4703-10. https://doi.org/10.1063/1.332803

Eringen, A.C. (1976), *Nonlocal Polar Field Models*, New York: Academic.

Faroughi, S. and Seyed Mohammad Hossein, G. (2016), "Analysis of axial vibration of non-uniform nanorod using boundary characteristic orthogonal polynomials", *Modares Mech. Eng.*, **16**, 203-212, http://mme.modares.ac.ir/article-15-528-en.html

Fernandes, R., El-Borgi, S. Mousavi, S.M., Reddy, J.N. and Mechmoum, A. (2017), "Nonlinear size-dependent longitudinal vibration of carbon nanotubes embedded in an elastic medium", *Physica E*, **88**, 18-25. https://doi.org/10.1016/j.physe.2016.11.007

Güven, U. (2014), "Love–Bishop rod solution based on strain gradient elasticity theory", *C.R. Mec*, **342**, 8-16. https://doi.org/10.1016/j.crme.2013.10.011

Gómez-Silva, F. and Zaera, R. (2022a), "Novel Enriched Kinetic Energy continuum model for the enhanced prediction of a 1D lattice with next-nearest interactions", *Compos. Struct.*, **281**, 115003. https://doi.org/10.1016/j.compstruct.2021.115003

Gómez-Silva, F. and Zaera, R. (2022b), "Low order nonstandard continualization of a beam lattice with next-nearest interactions, Enhanced prediction of the dynamic behavior", *Mech. Adv. Mater. Struct.*, **29**(27), 6216-6230. https://doi.org/10.1080/15376494.2021.1974616

Gómez-Silva, F. and Zaera, R. (2022c), "New low-order continuum models for the dynamics of a Timoshenko beam lattice with next-nearest interactions", *Comput Struct.*, **272**, 106864. https://doi.org/10.1016/j.compstruc.2022.106864

Hainfeld, J.F., Dilmanian F.A., Zhong Z., Daniel N.S., John A.K. and Henry, M.S. (2010), "Gold nanoparticles enhance the radiation therapy of a murine squamous cell carcinoma", *Phys. Med. Biol.* **55**, 3045. https://doi.org/10.1088/0031-9155/55/11/004

He, Y.Q., Shao, P.L., Ling, K. and Zhong, F.L. (2005), "A study on the sizes and concentrations of gold nanoparticles by spectra of absorption, resonance Rayleigh scattering and resonance non-linear scattering", *Spectrochim. Acta, Part A*, **61**, 2861-66. https://doi.org/10.1016/j.saa.2004.10.035

Hsu, J.C., Haw, L. and Win-Jin, C. (2011), "Longitudinal vibration of cracked nanobeams using nonlocal elasticity theory", *Curr. Appl. Phys.* **11**, 1384-1388. https://doi.org/10.1016/j.cap.2011.04.026

Karličić, D., Milan, C., Tony, M. and Sondipon A. (2015), "Nonlocal longitudinal vibration of viscoelastic coupled double-nanorod systems", *Eur. J. Mech. A. Solids* **49**, 183-196. https://doi.org/10.1016/j.euromechsol.2014.07.005

Kiani, K. (2010), "Free longitudinal vibration of tapered nanowires in the context of nonlocal continuum theory via a perturbation technique", *Physica E*, **43**, 387-97. https://doi.org/10.1016/j.physe.2010.08.022

Kik, P.G. and Mark, L.B. (2007), *Surface Plasmon Nano-photonics*, *Surface Plasmon Nanophotonics*, Springer Book.

Kumar, R., Binetti, L., Nguyen, T.H., Alwis, L.S., Agrawal, A., Sun, T. and Grattan, K.T. (2019), "Determination of the aspect-ratio distribution of gold nanorods in a colloidal solution using UV-visible absorption spectroscopy", *Sci. Rep.*, **9**(1), 17469.

Li, X.F., Zhi-Bin She, and Kang, Y.L. (2017), "Axial wave propagation and vibration of nonlocal nanorods with radial deformation and inertia", *ZAMM*, **97**, 602-616. https://doi.org/10.1002/zamm.201500186

Louis, C. and Olivier, P. (2012), *Gold Nanoparticles in the Past, Before the Nanotechnology Era*, *Gold Nanoparticles for Physics, Chemistry And Biology*, 1, Book.

Malekzadeh, P. and Karami, G. (2005), "Polynomial and harmonic differential quadrature methods for free vibration of variable thickness thick skew plates", *Eng Struct*, **27**, 1563-1574. https://doi.org/10.1016/j.engstruct.2005.03.017

Miller, K.D, Rebecca, L.S., Chun, C.L., Angela, B.M., Joan, L.K., Julia, H.R, Kevin, D.S., Rick, A. and Ahmedin, J. (2016), "Cancer treatment and survivorship statistics", *CA Cancer J Clin*, **66**, 271-289. https://doi.org/10.3322/caac.21349

Morton, J.G, Emily, S.D., Naomi, J.H. and Jennifer, L.W. (2010), *Nanoshells for Photothermal Cancer Therapy*, *Cancer nanotechnology*, Springer Book.

Mousavi, S.M, and Fariborz, S.J. (2012), *Free Vibration of a Rod Undergoing Finite Strain*, *Journal of Physics*, *Conference Series*, 012011. IOP Publishing.

Murmu, T, and Adhikari, S. (2010), "Nonlocal effects in the longitudinal vibration of double-nanorod systems", *Physica E*, **43**, 415-22. https://doi.org/10.1016/j.physe.2010.08.023

Murmu, T., Adhikari, S. and McCarthy, M.A. (2014), "Axial vibration of embedded nanorods under transverse magnetic field effects via nonlocal elastic continuum theory", *J. Comput. Theor. Nanosci.* **11**, 1230-1236. https://doi.org/10.1166/jctn.2014.3487

Narendar, S. and Gopalakrishnan, S. (2011), "Axial wave propagation in coupled nanorod system with nonlocal small scale effects", *Compos. Part B*, **42**, 2013-2023. https://doi.org/10.1016/j.compositesb.2011.05.021

Nayfeh, A.H. and Nayfeh, S.A. (1994), "On nonlinear modes of continuous systems", Tsukuba.

Nazemnezhad, R. and Kamran, K. (2018a), "An analytical study on the size dependent longitudinal vibration analysis of thick nanorods", *Mater. Res. Express* **5**, 075016. https://doi.org/10.1088/2053-1591/aacf6e/meta

Nazemnezhad, R. and Kamran, K. (2018b), "Free axial vibration analysis of axially functionally graded thick nanorods using nonlocal Bishop's theory", *Steel. Compos. Struct.*, **28**, 749-758. https://doi.org/10.12989/scs.2018.28.6.749

Nazemnezhad, R., Ruhollah, M. and Amin, S. (2019), "Surface energy effect on nonlinear free axial vibration and internal resonances of nanoscale rods", *Eur. J. Mech. A. Solids*, **77**, 103784. https://doi.org/10.1016/j.euromechsol.2019.05.001

Pitsillides, C.M., Joe, E.K., Wei, X. anderson, R.R. and Lin, C.P. (2003), "Selective cell targeting with light-absorbing micro-particles and nanoparticles", *Biophys. J.*, **84**(6), 4023-4032. https://doi.org/10.1016/S0006-3495(03)75128-5

Rao, S.S. (2019), *Vibration of Continuous Systems*, John Wiley & Sons, New York, U.S.A.

Saha, K., Sarit, S.A., Chaekyu, K., Xiaoning, L. and Vincent, M. R. (2012), "Gold nanoparticles in chemical and biological sensing", *Chem. Rev.*, **112**, 2739-2779. https://doi.org/10.1021/cr2001178

Shakhlavi, S.J., Hosseini-Hashemi, S. and Nazemnezhad, R. (2022a), "Thermal stress effects on size-dependent nonlinear axial vibrations of nanorods exposed to magnetic fields surrounded by nonlinear elastic medium", *J. Therm. Stress.*, **45**(2), 139-153. https://doi.org/10.1080/01495739.2021.2003275

Shakhlavi, S.J., Hosseini-Hashemi, S. and Nazemnezhad, R. (2022b), "Nonlinear nano-rod-type analysis of internal resonances and geometrically considering nonlocal and inertial effects in terms of Rayleigh axial vibrations". *Eur. Phys. J. Plus*, **137**(4), 1-20.

https://doi.org/10.1140/epjp/s13360-022-02594-x
Shakhlavi, S.J., Nazemnezhad, R., Hosseini-Hashemi, S. and Amabili, M. (2021a), "Analysis of nonlinear nonlocal axial free vibrations of gold nanoscale rod", *Proceedings of the 29th Annual International Conference of Iranian Association of Mechanical Engineers and 8th International Conference on Thermal Power Plants Industry*, Tehran.
Shakhlavi, S.J., Nazemnezhad, R., Hosseini-Hashemi, S. and Amabili, M. (2021b), "On nonlocal nonlinear internal resonances of gold nanoscale rod", *Proceedings of the 10th International Conference on Acoustics and Vibration*, Tehran.
Shakhlavi, S.J., Nazemnezhad, R. and Hosseini-Hashemi, S. (2020), "On nonlinear torsional vibrations of nanorod", *Proceedings of the 28th Annual Conference of Mechanical Engineering*, *Tehran*.
Shakhlavi, S.J. (2023), "On nonlinear damping effects with nonlinear temperature-dependent properties for an axial thermo-viscoelastic rod", *Int. J. Non Linear Mech*, **153**, 104418. https://doi.org/10.1016/j.ijnonlinmec.2023.104418
Shakhlavi, S.J., Shahrokh, H.H. and Nazemnezhad, R. (2020), "Torsional vibrations investigation of nonlinear nonlocal behaviour in terms of functionally graded nanotubes", *Int. J. Non Linear Mech*, 103513. https://doi.org/10.1016/j.ijnonlinmec.2020.103513
Shakhlavi, S.J. (2024), "Nonlinear nonlocal damping effects under magnetic loads of a ferromagnetic-viscoelastic nanotube exposed to a nonlinear elastic medium with nonlocal viscosity", *Commun*. *Nonlinear Sci*. *Numer*. *Simul*., **130**, 107690. https://doi.org/10.1016/j.cnsns.2023.107690
Shakhlavi, S.J. and Nazemnezhad, R. (2024), "Study on derivation from large amplitude size dependent internal resonances of homogeneous and FG rod-types", *Adv. Nano Res*, **16**(2), 111. https://doi.org/10.12989/anr.2024.16.2.111
Striz, A.G., Wang, X. and Bert, C.W. (1995), "Harmonic differential quadrature method and applications to analysis of structural components", *Acta Mech*., **111**, 85-94. https://doi.org/10.1007/BF01187729
Sun, Y. and Younan, X. (2003).'"Gold and silver nanoparticles, a class of chromophores with colors tunable in the range from 400 to 750 nm", *Analyst*, **128**, 686-91. https://doi.org/10.1039/B212437H

CC